

1 **Are recent changes in sediment manganese sequestration** 2 **in the euxinic basins of the Baltic Sea linked to the** 3 **expansion of hypoxia?**

4
5 **C. Lenz^{1,2}, T. Jilbert², D.J. Conley¹, M. Wolthers^{3,2} and C.P. Slomp²**

6 [1]{Department of Geology, Lund University, Sölvegatan 12, SE-22362 Lund, Sweden}

7 [2]{Department of Earth Sciences, Faculty of Geosciences, Utrecht University, Budapestlaan
8 4, 3584 CD Utrecht, the Netherlands}

9 [3]{University College London, Department of Chemistry, 20 Gordon Street, London, WC1H
10 0AJ, United Kingdom}

11 Correspondence to: C. Lenz (conny.lenz@geol.lu.se)

12 13 **Abstract**

14 Expanding hypoxia in the Baltic Sea over the past century has led to anoxic and sulfidic
15 (euxinic) deep basins that are only periodically ventilated by inflows of oxygenated waters
16 from the North Sea. In this study, we investigate the potential consequences of the expanding
17 hypoxia for manganese (Mn) burial in the Baltic Sea using a combination of pore water and
18 sediment analyses of dated sediment cores from 8 locations. Diffusive fluxes of dissolved Mn
19 from sediments to overlying waters at oxic, hypoxic and euxinic sites are in line with an
20 active release of Mn from these areas. Although the fluxes are significant (ranging up to ca.
21 $240 \mu\text{mol m}^{-2} \text{d}^{-1}$), published water column data suggest that the benthic release of Mn is
22 small when compared to the large pool of Mn already present in the hypoxic and anoxic water
23 column. Our results highlight two modes of Mn carbonate formation in sediments of the deep
24 basins. In the Gotland Deep area, Mn carbonates likely form from Mn oxides that are
25 precipitated from the water column directly following North Sea inflows. In the Landsort
26 Deep, in contrast, Mn carbonate and Mn sulfide layers appear to form independent of inflow
27 events, and are possibly related to the much larger and continuous input of Mn oxides linked
28 to sediment focusing. While formation of Mn enrichments in the Landsort Deep continues to
29 the present, this does not hold for the Gotland Deep area. Here, a recent increase in euxinia, as

1 evident from measured bottom water sulfide concentrations and elevated sediment
2 molybdenum (Mo), coincides with a decline in sediment Mn. Sediment analyses also reveal
3 that recent inflows of oxygenated water (since ca. 1995) are no longer consistently recorded
4 as Mn carbonate layers. We hypothesize that the recent rise in sulfate reduction rates linked to
5 eutrophication and decline in reactive Fe input to these basins, as recorded by sediment Fe/Al
6 ratios, has led to higher sulfide availability near the sediment-water interface after inflow
7 events. As a consequence, the Mn oxides may be reductively dissolved more rapidly than in
8 the past and Mn carbonates may no longer form. Using a simple diagenetic model for Mn
9 dynamics in the surface sediment, we demonstrate that an enhancement of the rate of
10 reduction of Mn oxides is in line with such a scenario. Our results have important
11 implications for the use of Mn carbonate enrichments as a redox proxy in marine systems.

12

13 **1 Introduction**

14 Manganese (Mn) enrichments in brackish and marine sedimentary deposits can be used as an
15 indicator of redox changes in the overlying waters (e.g. Calvert and Pedersen, 1993). In
16 anoxic settings, Mn-enrichments are typically assumed to consist of Mn carbonates, which are
17 associated with calcium and can contain other impurities (e.g. Jakobsen and Postma, 1989;
18 Manheim, 1961; Sternbeck and Sohlenius, 1997; Suess, 1979). For simplicity, in this study
19 these phases are collectively referred to as Mn carbonates, despite their obvious greater
20 complexity and heterogeneity. Mn carbonate minerals are suggested to form from Mn oxides
21 deposited during periods of bottom water oxygenation (Calvert and Pedersen, 1996;
22 Huckriede and Meischner, 1996), with Mn^{2+} availability thought to be the key control
23 (Neumann et al., 2002). However, sediment Mn data for both the Landsort Deep in the Baltic
24 Sea (Lepland and Stevens, 1998) and the Black Sea (Lyons and Severmann, 2006) indicate
25 that Mn enrichments may also form in sediments overlain by continuously anoxic bottom
26 waters. In the Landsort Deep, these enrichments consist of both Mn carbonates and Mn
27 sulfides (Lepland and Stevens, 1998; Suess, 1979). The formation of Mn carbonate is
28 assumed to be driven by an exceptionally high alkalinity. Mn sulfides form when H_2S exceeds
29 Fe availability (Böttcher and Huckriede, 1997; Lepland and Stevens, 1998). Some Mn may
30 also be incorporated in pyrite (e.g. Huerta-Diaz and Morse, 1992; Jacobs et al., 1985), but the
31 amounts are relatively minor when compared to those present in Mn carbonate as shown in a
32 recent study for Baltic Sea sediments (Lenz et al., 2014). Finally, Mn enrichments may also

1 form in sediments overlain by oxic bottom waters upon increased input and precipitation of
2 Mn oxides and transformation to Mn carbonate during burial (e.g. MacDonald and Gobeil,
3 2012). A better understanding of the various modes of formation of sedimentary Mn and the
4 link with variations in bottom water redox conditions is essential when interpreting Mn
5 enrichments in geological deposits (e.g. Calvert and Pedersen, 1996; Huckriede and
6 Meischner, 1996; Jones et al., 2011; Meister et al., 2009).

7 Redox-dependent dynamics of Mn have been studied extensively in the Baltic Sea (e.g.
8 Huckriede and Meischner, 1996; Lepland and Stevens, 1998; Neumann et al., 2002) and are
9 of interest because of the large spatial and temporal variations in bottom water oxygen
10 conditions over the past century that are particularly well documented since the 1970's
11 (Fonselius and Valderrama, 2003). Besides providing evidence for sporadic inflows of
12 oxygenated saline water from the North Sea that affect brackish bottom waters in all deep
13 basins (Matthäus and Franck, 1992; Matthäus et al. 2008), the available hydrographic data
14 indicate a major expansion of the hypoxic area in the Baltic Sea linked to increased
15 eutrophication (Carstensen et al., 2014; Conley et al., 2009; Gustafsson et al., 2012; Savchuk
16 et al., 2008). While the shallower areas in the Baltic Sea are now seasonally hypoxic, the deep
17 basins all show a major shift towards anoxic and sulfidic (euxinic) conditions around 1980
18 (Fonselius and Valderrama, 2003; Mort et al., 2010). These basin-wide changes in redox
19 conditions likely had a major impact on both the sources and sinks of sediment Mn in the
20 Baltic Sea.

21 River input (Ahl, 1977; Martin and Meybeck, 1979) and release from sediments (Sundby et
22 al., 1981; Yeats et al., 1979) are the key sources of Mn in the water column of marine coastal
23 basins. While in areas with oxic bottom waters, dissolved Mn produced in the sediment will
24 mostly be oxidized to Mn oxide in the surface layer and thus will be trapped in the sediment,
25 dissolved Mn may escape to the overlying water when the oxic surface layer is very thin
26 (Slomp et al., 1997). In the water column, this Mn may be oxidized again (e.g. Dellwig et al.,
27 2010; Turnewitsch and Pohl, 2010) and contribute to the depositional flux of Mn oxides
28 (Mouret et al., 2009), or may be laterally transferred in dissolved or particulate form. The
29 lateral transfer of Mn from oxic shelves to deep basins, where the Mn may be trapped and
30 ultimately may precipitate as authigenic minerals, is termed the "Mn shuttle" (Lyons and
31 Severmann, 2006).

1 During the expansion of hypoxia and anoxia, as observed in the Baltic Sea over the past
2 century (Conley et al., 2009), the Mn shuttle likely became more efficient in transporting Mn
3 to deeper, euxinic basins because of decreased trapping of Mn in oxygenated surface
4 sediments (Lyons and Severmann, 2006). However, during an extended period of hypoxia and
5 anoxia, sediments in hypoxic areas may become depleted of Mn oxides, thus reducing the
6 strength of the Mn shuttle from oxic and hypoxic shelves to the deep basins. In addition, the
7 formation rate of authigenic Mn minerals in the sediment at deep basin sites may change in
8 response to bottom water hypoxia and anoxia. If release of dissolved Mn^{2+} from Mn oxides –
9 formed at the sediment surface following inflows of oxygenated North Sea water – is the
10 dominant control for Mn carbonate formation in the sediment as suggested for the Gotland
11 Deep (Neumann et al., 2002), expanding bottom water anoxia might allow Mn oxides to be
12 reduced in the water column and at the sediment-water interface, precluding conversion to Mn
13 carbonates. This mechanism was recently invoked to explain the lack of Mn carbonates in the
14 sediment during periods of bottom water euxinia in the Gotland Deep during the Holocene
15 Thermal Maximum (Lenz et al., 2014). If alkalinity is the key control, however, as suggested
16 for the Landsort Deep (Lepland and Stevens, 1998), Mn sequestration would be expected to
17 be similar or increase due to higher rates of sulfate reduction.

18 In this study, we use geochemical analyses of dated sediment cores for 8 sites in the Baltic
19 Sea, combined with pore water data to assess the role of variations in water column redox
20 conditions for Mn dynamics in surface sediments in the Baltic Sea. We capture the full range
21 of redox conditions (oxic, hypoxic and euxinic) to investigate the cycling of Mn in the
22 sediment, the present-day diffusive flux from the sediments and the sequestration of Mn in
23 mineral phases. While the pore water data only provide a “snapshot” of the conditions at the
24 time of sampling, the sediment data in the euxinic basins record both the expansion of
25 hypoxia and anoxia and the effects of short-term inflows of oxygenated North Sea water. Our
26 results indicate release of Mn from oxic and hypoxic areas as well as the deep basin sites, and
27 sequestration of Mn carbonates and sulfides in the Landsort Deep. The lack of recent Mn
28 accumulation at various deep basin sites suggests that inflows of oxygenated seawater are no
29 longer consistently recorded by Mn carbonate deposits in these settings.

1 **2 Materials and Methods**

2 **2.1 Study area**

3 Fine-grained sediments from 8 locations in the southern and central Baltic Sea were collected
4 during 4 cruises between 2007 and 2011 (Figure 1, Table 1) using a multi-corer. The sites
5 differ with respect to their water depths and their present-day bottom water redox conditions.
6 The Fladen and LF1 sites are located in the Kattegat and along the eastern side of the Gotland
7 Deep, respectively, and are fully oxic, whereas site BY5 in the Bornholm Basin is seasonally
8 hypoxic (Jilbert et al., 2011; Mort et al., 2010). The remaining stations, LF3, LL19, BY15
9 (Gotland Basin), F80 (Fårö Deep) and LD1 (Landsort Deep), are situated below the
10 redoxcline, which was located between 80 and 120 m water depth at the time of sampling.
11 Therefore, bottom waters at these sites were all anoxic and sulfidic (euxinic). The latter 4 sites
12 are located in the deep central basins of the Baltic Sea, at water depths ranging from 169 m at
13 LL19 to 416 m at LD1. Water column data for oxygen and hydrogen sulfide for LL19 and
14 LD1 (as recorded at LL23 as a nearby station) are available from the ICES Dataset on Ocean
15 Hydrology (2014). The sampling, and selected pore water and sediment analyses for many of
16 our sites have been described previously (Mort et al., 2010, Jilbert et al., 2011; Jilbert and
17 Slomp, 2013a). For completeness, all procedures are described again below.

18 **2.2 Bottom water and pore water analyses**

19 A bottom water sample was taken from the water overlying the sediment in each multicore as
20 soon as possible after core collection. At each site, sediment multi-cores (<50 cm, 10 cm i.d.)
21 were either immediately sectioned in a N₂-filled glovebox at in-situ temperature or sampled
22 with syringes through pre-drilled holes in the core liner. A small portion of each sample was
23 stored at 5°C or -20°C in gas-tight jars for sediment analyses. The remaining sediment was
24 centrifuged (10-30 min.; 2500 g) in 50 ml greiner tubes to collect pore water. Both the pore
25 water and a bottom water sample were filtered (0.45 µm pore size) and subdivided for later
26 laboratory analyses. All pore water handling prior to storage was performed in a N₂
27 atmosphere. A subsample of 0.5 ml was directly transferred to a vial with 2 ml of a 2% Zn-
28 acetate solution for analysis of hydrogen sulfide. Sulfide concentrations were determined by
29 complexation of the ZnS precipitate using phenylenediamine and ferric chloride (Strickland
30 and Parsons, 1972). Subsamples for total Mn, Fe, Ca and S were acidified with either HNO₃
31 (Fladen, BY5) or HCl (all other stations) and stored at 5°C until further analysis with

1 Inductively Coupled Plasma – Optical Emission Spectroscopy (ICP-OES; Perkin Elmer
2 Optima 3000; relative precision and accuracy as established by standards (ISE-921) and
3 duplicates were always <5%). Hydrogen sulfide was assumed to be released during the initial
4 acidification, thus S is assumed to represent SO_4^{2-} only. Total Mn and Fe are assumed to
5 represent Mn^{2+} and Fe^{2+} although in the former case some Mn^{3+} may also be included
6 (Madison et al., 2011). Subsamples for NH_4 were frozen at -20°C until spectrophotometric
7 analysis using the phenol hypochlorite method (Riley, 1953). A final subsample was used to
8 determine the pH with a pH electrode and meter (Sentron). Note that degassing of CO_2 may
9 impact ex-situ pH measurements and may lead to a rise in pH (Cai and Reimers, 1993). As a
10 consequence, our pH values should be seen as an approximation only. The total alkalinity was
11 then determined by titration with 0.01 M HCl. All colorimetric analyses were performed with
12 a Shimadzu spectrophotometer. Replicate analyses indicated that the relative error for the pore
13 water analyses was generally <10 %.

14 At four deep basin sites (LL19, BY15, F80, LD1), a second multicore was sampled and
15 analysed for methane as described by Jilbert and Slomp (2013a). Briefly, a cutoff syringe was
16 inserted into a pre-drilled, taped hole at 1.5 cm intervals directly after core collection.
17 Precisely 10 ml wet sediment was extracted from each hole and transferred immediately to a
18 65 ml glass bottle filled with saturated sodium chloride (NaCl) solution. This bottle was then
19 closed with a rubber stopper and screwcap, and a headspace of 10 ml N_2 gas was inserted.
20 Methane concentrations in the headspace of the glass bottles were determined by injection of
21 a subsample into a Thermo Finnigan Trace GC gas chromatograph (flame ionization detector,
22 Restek Q-PLOT column of 30 m length, 0.32 mm internal diameter, oven temperature 25°C).
23 Data were then back-calculated to the original pore water concentrations using the measured
24 porosities (see Section 2.3). Because of degassing, which is unavoidable at sites with very
25 high CH_4 concentrations, the CH_4 profile at LD1 is considered to be less reliable

26 **2.3 Sediment analyses**

27 Sediment samples were freeze-dried and water contents and porosities were calculated from
28 the weight loss, assuming a sediment density of 2.65 g cm^{-3} . Sediments were then ground in
29 an agate mortar in a N_2 or argon-filled glovebox. From each sediment sample, aliquots for
30 several different analyses were taken. For total organic carbon (TOC) analyses, 0.3 g of
31 sediment was decalcified with 1M HCl and the C content was determined with a Fisons NA
32 1500 CNS analyser (van Santvoort et al., 2002). Based on the analyses of laboratory reference

1 materials and replicates, the relative error of the TOC measurements was generally less than
2 5%. Total sediment contents of S, Mn, Ca, Fe, Al and Mo were determined by ICP-OES, after
3 dissolution of 0.125 g of sample with an HF/HClO₄/HNO₃ mixture in closed Teflon bombs at
4 90°C, followed by evaporation of the solution and redissolution of the remaining gel in 1M
5 HNO₃ (Passier et al., 1999). The accuracy and precision of the measurements were
6 established by measuring laboratory reference materials (ISE-921 and in-house standards) and
7 sample replicates; relative errors were <5% for all reported elements. The detection limits of
8 ICP-OES for Mn, Mo, Ca, Fe, Al and S in the HNO₃ solution are 0.6, 14, 5, 6 and 24 µg kg⁻¹
9 and 0.28 mg kg⁻¹ respectively. All elemental concentrations in the sediment were corrected for
10 the weight of the salt in the pore water using the ambient salinity and porosity.

11 Age models based on ²¹⁰Pb analyses for 6 multi-cores used in this study have been previously
12 published. For details, we refer the reader to the relevant studies: Fladen and BY5 (Mort et al.,
13 2010), LF1 and LF3 (Jilbert et al., 2011), LL19 (Zillén et al., 2012) and BY15 (Jilbert and
14 Slomp, 2013b). A new ²¹⁰Pb age model was constructed for LD1. Samples from the Landsort
15 Deep (LD1) were analyzed with a Canberra BeGe gamma ray spectrometer at Utrecht
16 University. The samples were freeze-dried, homogenized, and transferred into vent-free petri
17 dishes, which were sealed in polyethylene bags and stored for 2 weeks before measuring.
18 Each sample was measured until 200-250 ²¹⁰Pb gamma-ray counts were reached. For the age
19 determination a constant rate of supply model (Appleby and Oldfield, 1983) was implemented
20 using a background estimated from the mean counts of ²¹⁴Pb and ²¹⁴Bi. For further details on
21 the age models and the ²¹⁰Pb data for LD1, we refer to the supplementary information
22 Appendix A. The age model for the site in the Fårö Deep (F80) was constructed using high
23 resolution Mo and Mn data. In 2013, an extra sediment core from this station was taken. Mini
24 sub-cores as described in section 2.4 were embedded in Spurr's epoxy resin and measured by
25 Laser Ablation - Inductively Coupled Plasma – Mass Spectrometry (LA-ICP-MS) line
26 scanning. The fluctuations in Mo/Al and Mn/Al ratios were coupled to the instrumental
27 records of bottom water oxygen conditions. The 2009 multicore profiles were subsequently
28 tuned to the dated profiles from 2013 (see Appendix A for more details).

29 **2.4 Microanalysis**

30 Mini sub-cores of 1 cm diameter and up to ~12 cm length each were taken from the top part
31 of sediment multicores at sites LL19 and LD1 in May 2011 as described in detail by Jilbert
32 and Slomp (2013b). Briefly, the pore water was replaced by acetone and the sub-core was

1 fixed in Spurr's epoxy resin. During the whole procedure the sub-cores remained upright.
2 During the dewatering process the sediment compacted resulting in a reduction of length of
3 both sections by up to 50%. After curing, epoxy-embedded sub-cores were opened
4 perpendicular to the plane of sedimentation and the exposed internal surface was polished.

5 Line scans were performed with LA-ICP-MS, to measure high-resolution vertical profiles of
6 selected elements in the resin blocks of the two cores. A Lambda Physik laser of wavelength
7 193 nm and pulse rate of 10 Hz was focused onto the sample surface with a spot size of 120
8 μm . During line scanning, the sample was moved under the laser beam with a velocity of
9 0.0275 mm/s, creating an overlapping series of pulse craters. From the closed sample chamber
10 the ablated sample was transferred to a Micromass Platform ICP-MS by He-Ar carrier gas.
11 Specific isotopes of aluminum (^{27}Al), iron (^{57}Fe), manganese (^{55}Mn), sulfur (^{34}S) and
12 molybdenum (^{98}Mo) were measured. For site LD1, bromine (^{81}Br) was also measured. LA-
13 ICP-MS data for each element were calibrated by reference to the sensitivities (counts/ppm)
14 of the glass standard NIST SRM 610 (Jochum et al., 2011) and corrected for the natural
15 abundances of the analyzed isotopes. All data are reported normalized to Al to correct for
16 variations in sample yield. For S/Al data, a further sensitivity factor was applied which
17 compensates for the contrasting relative yield of S from NIST SRM 610 with respect to
18 embedded sediments.

19 The resin-embedded samples were also mounted inside an EDAX Orbis Micro XRF Analyzer
20 to construct elemental maps at a spatial resolution of 30 μm for manganese (Mn), calcium
21 (Ca) and sulfur (S) (Micro XRF settings: Rh tube at 30 kV, 500 μA , 300 ms dwell time, 30
22 μm capillary beam).

23 To allow comparison of the data from the micro analyses with the discrete samples, the
24 measured profiles of the LA-ICP-MS were expanded to the original length of the core section
25 and aligned to the discrete sample data (not shown).

26 **2.5 Flux calculations**

27 The diffusive flux of manganese across the sediment-water interface (J_{sed}) was calculated
28 from the concentration gradient in the pore water over the upper 0.25 to 2.5 cm of the
29 sediment with Fick's first law for 6 sites:

$$30 \quad J_{\text{sed}} = -\phi D_{\text{sed}} \frac{dC_{\text{Mn}^{2+}}}{dx} \quad (1)$$

1 where ϕ is the porosity (as listed in Appendix B), D_{sed} is the whole sediment diffusion
2 coefficient for dissolved Mn^{2+} , C is the dissolved Mn^{2+} concentration and x is depth in the
3 sediment. D_{sed} was calculated from the diffusion coefficient of Mn^{2+} in free solution corrected
4 for ambient salinity and temperature (D_{SW}) and porosity (Boudreau, 1997):

$$5 \quad D_{\text{sed}} = \frac{D_{\text{SW}}}{(1 - \ln \phi^2)} \quad (2)$$

6 Whenever possible (LL19, BY15 and F80) higher resolution data from the 2009 Aranda
7 cruise was used for the calculation (Table 2 and data in Appendix B).

8 **2.6 Saturation state**

9 Thermodynamic equilibrium calculations were performed for the pore water of LF3, LL19,
10 BY15, F80 and LD1 using version 3.1.1 of the computer program PHREEQC (Parkhurst and
11 Appelo, 1999) with the LLNL database. Our calculations should be seen as approximations
12 with the main purpose of providing a comparison to previous calculations by Carman and
13 Rahm (1997) and Heiser et al. (2001) to assess whether there are any indications for a change
14 in saturation state of the pore water between inflows. The LLNL database does not contain the
15 authigenic carbonate phases present in the Baltic Sea. However, data from the literature
16 (Jakobsen and Postma, 1989; Sternbeck and Sohlenius, 1997; Lepland and Stevens, 1998;
17 Huckriede and Meischner 1996; Kulik et al., 2000) suggest that Baltic carbonates are
18 predominantly Mn carbonates with a substantial contribution of Ca. Therefore, an
19 approximation of the solubility product of (Mn, Ca) CO_3 solid solutions was generated using
20 the equations given in Katsikopoulos et al. (2009). The stoichiometric solubility product (K_{st})
21 was calculated using $\text{Mn}_{0.74}\text{Ca}_{0.26}\text{CO}_3$ (Kulik et al 2000) as a common ratio measured for
22 (Mn, Ca) CO_3 solid solutions in Baltic Sea sediments.

23 An equilibrium constant pK of 0.377 (Emerson et al. 1983) was used for Mn sulfide. The
24 solubility of iron sulfide from Rickard (2006) was added to the calculations as well as MnHS^+
25 as a solute (Luther et al., 1996) because it is likely abundant in pore water in sulfidic
26 sediments (Heiser et al., 2001). At sites LF3 and LD1, Fe^{2+} was below the detection limit and
27 the calculation of the saturation state with respect to FeS could not be performed. Carbonate
28 alkalinity was calculated from titration alkalinity as described by Carman and Rahm (1997).

1 2.7 Diagenetic model for Mn

2 A simple diagenetic model for Mn was developed to assess the potential effect of changes in
3 the kinetics of reductive dissolution of Mn oxides to dissolved Mn^{2+} and subsequent Mn
4 carbonate formation in Baltic Sea surface sediments following an inflow event. Our modeling
5 is generic and addresses this research question only. Therefore, we do not attempt to describe
6 all the relevant processes potentially controlling Mn carbonate formation in the sediment nor
7 do we focus on a specific location. The model accounts for two biogeochemical processes:
8 reductive dissolution of Mn oxides to Mn^{2+} and precipitation of Mn^{2+} in the form of Mn
9 carbonates. Empirical rate laws for Mn oxide reduction and Mn carbonate formation are
10 assumed, with rates depending on first order rate constants for both processes (k_{red} and k_{prec})
11 and the sediment concentration of Mn oxide and dissolved Mn^{2+} , respectively (Berner, 1980;
12 Slomp et al., 1997). Transport is assumed to occur through diffusion (Mn^{2+}) and sediment
13 burial (Mn^{2+} and both solids). Porosity (ϕ), temperature, sediment density (ρ_s) and rates of
14 sedimentation (ω) are assumed constant with depth and time. The following differential
15 equations were used:

$$16 \quad \frac{\partial C_{Mn^{2+}}}{\partial t} = D_{Mn^{2+}} \frac{\partial^2 C_{Mn^{2+}}}{\partial x^2} - \omega \frac{\partial C_{Mn^{2+}}}{\partial x} - k_{prec} C_{Mn^{2+}} + \frac{\rho_s(1-\phi)}{\phi} k_{red} C_{Mn_{oxide}} \quad (3)$$

$$17 \quad \frac{\partial C_{Mn_{oxide}}}{\partial t} = -\omega \frac{\partial C_{Mn_{oxide}}}{\partial x} - k_{red} C_{Mn_{oxide}} \quad (4)$$

$$18 \quad \frac{\partial C_{MnCO_3}}{\partial t} = -\omega \frac{\partial C_{MnCO_3}}{\partial x} + \frac{\phi}{\rho_s(1-\phi)} k_{prec} C_{Mn^{2+}} \quad (5)$$

19 where $C_{Mn^{2+}}$, $C_{Mn_{oxide}}$ and C_{MnCO_3} are the concentrations of dissolved Mn^{2+} , Mn oxides and
20 $MnCO_3$, respectively and $D_{Mn^{2+}}$ is the diffusion coefficient of dissolved Mn^{2+} as defined in
21 equation (2). The model code was written in R using the marelac (Soetaert et al., 2010) and
22 ReacTran (Soetaert and Meysman, 2012) packages. The model domain is represented by a
23 one-dimensional grid of 1000 cells that captures the interval from the sediment-water
24 interface to a depth of 1 cm. Environmental parameters typical for surface sediments in the
25 deep basins of the Baltic Sea and boundary conditions were assumed as defined in Table 3.

26 Here, we assess a scenario for Baltic Sea sediments where Mn oxides are deposited during a
27 period of oxic bottom water conditions for 4 months directly after a North Sea inflow
28 followed by a period of two months in which no Mn oxides are deposited because of the

1 return of bottom water anoxia (Table 3; Section 4.1). We set k_{prec} to $5,000 \text{ yr}^{-1}$, placing the
2 maximum rate of Mn carbonate formation in the model calculations in the upper range given
3 by Wang and Van Cappellen (1996). We then assess the response of benthic fluxes of Mn^{2+} ,
4 rates of formation of Mn carbonate in the sediment and profiles of the various Mn forms to
5 variations in k_{red} when assuming values of either 0.1, 1, 10, 100 or 1000 yr^{-1} during 4 months
6 of the simulation followed by a period of two months with a k_{red} of 1000 yr^{-1} (i.e. representing
7 rapid Mn oxide reduction after the return of anoxic conditions). By varying k_{red} , we wish to
8 capture a wide range in the availability of reductants for Mn oxides in the surface sediment.
9 Values of k_{red} estimated for different sedimentary environments overlain by oxic bottom
10 waters in the North Sea range from $0.04 - 150 \text{ yr}^{-1}$ (Slomp et al., 1997). The slightly wider
11 range assumed here is reasonable because of the more important role of anaerobic pathways
12 of organic matter degradation in deep basin sediments of the Baltic Sea sediments compared
13 to those in the North Sea (e.g. Mort et al., 2010 versus Slomp et al., 1997). To assess the
14 robustness of our results, we also perform the same simulations with even higher k_{prec} values
15 (up to $30,000 \text{ yr}^{-1}$).

16 **3 Results**

17 At the time of sampling, bottom waters were oxic at the Fladen and LF1 sites in the eastern
18 Gotland Basin, hypoxic at the Bornholm Basin site BY5, and anoxic and sulfidic at all other
19 locations (Table 1). Pore water Mn^{2+} concentrations increase with depth in the sediment at
20 most sites (Figure 2; Appendix B). At the Fladen site, however, Mn^{2+} concentrations decrease
21 again below ca. 5 cm and at the eastern Gotland Basin sites LF1 and LF3, Mn^{2+}
22 concentrations are lower than at other sites. Pore water Fe^{2+} shows a subsurface maximum at
23 the Fladen and LF1 sites, but is low or absent in the pore water at all other sites. Pore water
24 Ca^{2+} concentrations show little change with depth and are in line with the salinity gradient in
25 the Baltic Sea. Alkalinity and ammonium concentrations increase with sediment depth
26 simultaneously with a decline in sulfate. CH_4 is present at depth where sulfate is depleted at
27 the sites in the Fårö Deep (F80) and Landsort Deep (LD1) (Appendix B). Similar to Ca^{2+} ,
28 sulfate concentrations in the bottom water at the different stations are in line with the salinity
29 gradient in the Baltic Sea (Table 1). Concentrations of hydrogen sulfide in the pore water > 2
30 mM are found at the Fårö Deep and Landsort Deep sites F80 and LD1. The pore waters are
31 supersaturated with respect to Mn carbonate below the surface sediment at the Landsort Deep.
32 The other hypoxic and anoxic sites except LF3 reach saturation only at greater depth. For Mn

1 sulfide, in contrast, supersaturation is only observed at the Landsort Deep site, LD1 (Figure 3)
2 and below 35 cm at site F80. Pore waters were supersaturated with respect to FeS at the sites
3 in the Northern Gotland Basin (LL19), in the Gotland Deep (BY15) and Fårö Deep (F80)
4 (Appendix B). Note that degassing of CO₂ during centrifugation may have led to a shift in pH
5 to higher values, thereby enhancing the degree of saturation with respect to carbonate and
6 sulfide minerals. However, an upward shift of ca. 0.5 pH units due to this effect would not
7 greatly affect the observed trends with depth and contrasts between stations in the calculated
8 saturation states presented. Calculated diffusive fluxes of Mn²⁺ vary from 81 to 236 μmol m⁻²
9 d⁻¹, with the highest efflux from the sediment being observed at the hypoxic Bornholm Basin
10 site BY5 and in the anoxic Landsort Deep (LD1)(Table 2).

11 Average sedimentation rates vary significantly between sites, with 3- to 4-fold higher rates at
12 Fladen and in the Landsort Deep (LD1) when compared to the oxic site in the eastern Gotland
13 Basin (LF1) and Bornholm Basin (BY5)(Table 1; Figure 4). Sediments are highly porous
14 (Appendix B) and rich in organic carbon (TOC) with maxima of ca. 5 wt% at the oxic sites
15 Fladen and LF1 and ca. 16 wt% at the anoxic sites (Figure 4). While changes in TOC with
16 depth at Fladen and LF1 are relatively small, distinct enrichments in TOC are observed in the
17 upper part of the sediment at all anoxic sites. High contents of total Al, which is a proxy for
18 clays, are in line with the presence of fine-grained sediments throughout the cores (Appendix
19 B). Total sulfur contents are low at Fladen, but are higher at all other sites, and show
20 considerable variation with depth in the sediment. Mn is enriched in the surface sediment at
21 Fladen, but is nearly absent at the LF1, BY5 and LF3 sites. At sites LL19, BY15 and F80, Mn
22 is present again but is mostly observed at greater depth in the sediment. The upper 30 cm of
23 the sediment at site LD1 is highly enriched in Mn. Sediment Ca is high at Fladen, is enriched
24 in the surface sediment at site LF1, is low at sites BY5, LF3 and LL19 and follows the pattern
25 in Mn at sites BY15, F80 and LD1. Sediment Fe typically ranges between 2 to 6 wt% and
26 there is a trend towards lower Fe contents in the upper 5 to 20 cm of the sediment, following
27 an initial maximum at the bottom of the TOC-rich interval at many sites (Appendix B). This
28 upward declining trend is even more apparent when the Fe contents are normalized to Al
29 (Figure 4). Sediment Mo is low at the Fladen, LF1, BY5 and LF3 sites but is enriched at the
30 other sites, where profiles largely follow those of TOC (Figure 4).

31 The LA-ICP-MS line-scans of resin-embedded surface sediments at site LL19 in the Northern
32 Gotland Basin (Figure 5A) support the results of the discrete sample analysis (Figure 4) and

1 confirm that there are very few Mn rich laminae in recent sediments at this location. While
2 most of the minor enrichments of Mn are correlated with Fe, S and Mo (Figure 5A), three
3 peaks (at 3.6, 3.9 and 4.6 cm) are independent of these elements, suggesting that these Mn
4 enrichments dominantly consist of carbonates. This is confirmed by the Micro-XRF maps
5 (Figure 5B) of the corresponding interval, which indicate coincident Mn and Ca-rich layers.
6 The maps show clear Mn carbonate layers at ~3.9 cm and ~4.6 cm. However, the third
7 enrichment at 3.6 cm is less continuous and is only represented by one spot in the map. The
8 two distinct Mn carbonate layers can be linked to inflow events in 1993 and 1997, using the
9 ^{210}Pb -based age model for this site, after correction for compaction of the sediment during
10 embedding.

11 In the surface sediments of the Landsort Deep site (LD1), in contrast, a large number of Mn
12 enrichments with much higher concentrations than at LL19 are observed (Figure 4 and 5).
13 The LA-ICP-MS line scans show that highest values often coincide with enrichments in S,
14 Mo and Br but are not related to maxima in Fe. The micro-XRF-maps of Mn, Ca and S
15 confirm that enrichments in Mn are present as discrete layers. The RGB (Mn, Ca, S)
16 composite reveals two different compositions for the Mn enrichments. The purple layers in
17 the RGB composite are a result of enrichments of Mn (red) and S (blue) in the same pixel,
18 suggesting the presence of Mn sulfide. However, other layers and spots are orange to yellow,
19 indicating coincident enrichments of Ca (green) and Mn, suggesting carbonate enrichments
20 (Figure 5B).

21 Benthic fluxes of Mn^{2+} and rates of Mn carbonate formation calculated with the diagenetic
22 model depend on the value of the rate constant for the reduction of Mn oxides (k_{red}) assumed
23 for the period with oxic (4 months) bottom waters. While benthic fluxes of Mn^{2+} increase
24 with increasing values of k_{red} , especially during the first 4 months of the simulation, rates of
25 Mn carbonate formation integrated with depth decrease (Figure 6). In runs with low values of
26 k_{red} , Mn carbonate is mostly formed in the 2-month anoxic phase. Corresponding profiles of
27 Mn oxides at the end of the 4 month oxic phase and of Mn carbonates at the end of both the
28 oxic and anoxic phases at 6 months illustrate the dependence of Mn carbonate formation in
29 the model on the rate of reduction of Mn oxides. Example profiles of Mn^{2+} at the start of the
30 anoxic phase are also shown. Runs with a higher rate constant for precipitation of Mn
31 carbonates (k_{prec}) lead to more sharply defined peaks in Mn carbonate and more Mn carbonate

1 formation at higher k_{red} values, but the same trends in fluxes and rates with varying k_{red} are
2 observed (not shown).

3 **4 Discussion**

4 **4.1 Sediment Mn cycling in the Baltic Sea**

5 Our results indicate major differences in Mn dynamics in the varied depositional settings of
6 the Baltic Sea. Although located in the Kattegat far from the euxinic basins, processes at the
7 Fladen site (Figure 2 and 3) can be used to illustrate the typical processes at oxic sites. Here,
8 Mn cycling is largely internal to the sediment and the Mn that is released to the pore water at
9 depth mostly reprecipitates upon upward diffusion into the oxic surface sediment. At the
10 hypoxic site in the Bornholm Basin (BY5) there is no clear sediment Mn enrichment but there
11 is release of dissolved Mn to the pore water, presumably due to dissolution of Mn oxides,
12 within the upper 15 cm of the sediment. At this site, the highest diffusive Mn flux from the
13 sediment to the water column was found (Table 2). At one of the sites on the slope of the
14 eastern Gotland Basin (LF1), there is a significant release of Mn^{2+} but the sediments at this
15 site are low in solid-phase Mn. This suggests that the source of Mn at this site may be of a
16 transient nature. Our results highlight that sediments in hypoxic areas may act as sources of
17 Mn to the water column, with subsequent lateral transfer potentially bringing this Mn to the
18 deep basins (Huckriede and Meischner, 1996; Jilbert and Slomp, 2013a; Lyons and
19 Severmann, 2006; Scholz et al., 2013).

20 The pore water profiles of the 4 anoxic sites in the various deep basins (LL19, BY15, F80,
21 and LD1) all are indicative of release of Mn to the pore water, either from reductive
22 dissolution of Mn oxides or dissolution of Mn carbonates due to undersaturation (e.g. Heiser
23 et al., 2001; Jilbert and Slomp, 2013a). As a result, diffusive Mn fluxes from the sediment to
24 the water column are also observed at all these deep basin sites. However, the Mn released to
25 these deep waters remains trapped below the redoxcline in the water column. Although
26 reoxidation of the Mn and formation of mixed phases of Mn oxides and Fe-(III)-associated
27 phosphates upon upward diffusion of Mn into the redoxcline occurs (Dellwig et al., 2010;
28 Turnewitsch and Pohl, 2010), sinking of these phases into sulfidic waters leads to subsequent
29 reductive redissolution.

30 Due to the seasonal and inflow-related changes in redox conditions in the Baltic Sea, the lack
31 of detailed data sets on Mn^{2+} concentrations in the water column, and our very limited number

1 of study sites, we cannot accurately estimate the different reservoirs of Mn and the
2 importance of the present-day source of Mn from sediments overlain by oxic and hypoxic and
3 anoxic bottom waters at the basin scale. Nevertheless, we will attempt to make a rough
4 quantification using the data that is available and will then compare it to estimates from the
5 literature.

6 Taking an average deep water volume of 2,000 km³ and average hypoxic area of 47,000 km²
7 (Carstensen et al., 2014) and a deep water concentration of Mn of 8 μM (Löffler et al. 1997 as
8 cited by Heiser et al., 2001), the amount of Mn in the deep water is estimated at 1.6 x 10¹⁰
9 mol or 0.33 mol m⁻². The range in Mn fluxes in our study (0 to 236 μmol m⁻² d⁻¹; Table 2) is
10 comparable to benthic fluxes measured with in-situ chambers in other areas of the Baltic Sea
11 (e.g. the Gulf of Finland; Pakhomova et al., 2007) and estimated from pore water profiles
12 from the 1990's (e.g. Heiser et al., 2001). If we assume that a flux of ca. 90 μmol m⁻² d⁻¹ is
13 representative for the sediments overlain by hypoxic and anoxic bottom waters (Table 2;
14 based on the fluxes for LL19, F80 and BY15), we calculate a yearly flux of 0.033 mol m⁻²
15 from those sediments, which is equivalent to 10% of the inventory in the water column. In
16 similar calculations, Heiser et al. (2001) estimated the amount of Mn in the Gotland Deep to
17 be equal to 0.8 mol m⁻². With our estimate of the benthic flux, this would lead to a
18 contribution of the benthic flux of less than 5%.

19 Note, however, that the role of the benthic flux of Mn from hypoxic sediments will vary
20 spatially and may be biased towards high values because of preferential sampling of sites with
21 a relatively high sediment accumulation rate in most pore water studies. This may explain the
22 one order of magnitude lower benthic fluxes of Mn reported for the Gotland Deep area in
23 1999-2001 of ca. 7-8 μmol m⁻² d⁻¹ by Neretin et al. (2003) when compared to those in our
24 study (Table 2).

25 Benthic fluxes of Mn are also expected to be high upon the reestablishment of bottom water
26 anoxia after an inflow and then decline with time (Neretin et al., 2003). The exact impact of
27 inflows on the oxygenation of the bottom waters in the deep basins of the Baltic Sea varies
28 from site to site, however, and depends on the volume and oxygen content of the inflowing
29 water, its pathway and the oxygen concentration in the receiving basin (e.g. Carstensen et al.,
30 2014), with the general flow of water in the deep basins going from the Gotland to the Fårö
31 and the Landsort Deep (Holtermann et al., 2012). For example, the bottom water in the
32 Gotland Deep was free of hydrogen sulfide for 4 months following the inflow of 1993-1994

1 (Neretin et al., 2003; Yakushev et al., 2011) whereas the Landsort Deep was less affected
2 because the bottom water at the time contained oxygen already (Figure 7). Using
3 biogeochemical modeling of a typical inflow in the Gotland Deep area, Yakushev et al.
4 (2011) showed that dissolved Mn^{2+} in the water column was oxidized to Mn oxides and
5 settled to the bottom over a time period of months. Dissolved Mn^{2+} appeared in the water
6 column again upon the return of bottom water anoxia and steady state conditions in the water
7 column were established in the model after ca. 1.5 years.

8 In their study, Yakushev et al. (2011) concluded that sediments play only a minor role as a
9 source of Mn a few years after an inflow. Likely, the large pool of Mn in the water column of
10 the deep basins was mostly released from the formerly oxic sediments during the initial
11 expansion of hypoxia during the 20th century. Based on the fact that, apart from the changes in
12 Mn inventory between inflows, there is no clear trend in water column Mn concentrations in
13 the Baltic Sea with time over recent decades (Pohl and Hennings, 2005), it is likely that the
14 present-day Mn shuttling from the oxic and hypoxic areas around the deep basins is not as
15 important quantitatively as a source of Mn to the deep basins as it was at the onset of hypoxia
16 early in the 20th century.

17 Notably, Yakushev et al. (2011) consider Mn^{3+} besides Mn^{2+} in their model for
18 biogeochemical dynamics in the water column in the Gotland Deep. Dellwig et al. (2012)
19 found recently that Mn^{3+} is an important component in the water column Mn cycle in the
20 Landsort Deep but not in the Gotland Deep. Further work is required to elucidate the potential
21 importance of this finding to Mn dynamics in the Baltic Sea and its impact on other
22 biogeochemical cycles (e.g. Pakhomova and Yakushev, 2013) and to determine whether Mn^{3+}
23 plays a role in the sediments as well and impacts Mn sequestration (e.g. Madison et al., 2011).
24 Field studies of Mn dynamics in the water column and sediment during and directly after an
25 inflow would be of particular value.

26 **4.2 Manganese sequestration in the anoxic basins**

27 Formation of Mn bearing carbonates in the Gotland Basin and Landsort Deep is generally
28 described as being ubiquitous after inflows (e.g. Jakobsen and Postma, 1989). Between
29 inflows, when bottom waters in the deep basins of the Baltic Sea are anoxic, pore waters in
30 the surface sediments are typically assumed to be undersaturated with respect to Mn
31 carbonates down to a depth of ~5 to 8 cm based on saturation state calculations for idealized

1 minerals (Figure 3)(Carman and Rahm, 1997; Heiser et al., 2001). The dissolution of Mn
2 oxides in the surface sediment following an inflow of oxygenated North Sea water is thought
3 to lead to high Mn²⁺ concentrations in the pore water and strong oversaturation with respect to
4 Mn carbonates, although this has not been proven (Huckriede and Meischner, 1996;
5 Sternbeck and Sohlenius, 1997, Heiser et al., 2001). Various authors have correlated such
6 inflow events to specific accumulations of Mn carbonate in sediments of the Gotland Basin
7 (e.g. Heiser et al., 2001; Neumann et al., 1997). We observe such enrichments in all our deep
8 basin cores, with the magnitude of the enrichment increasing with water depth (Figure 4). We
9 suggest that this water depth effect between the deep basin sites is due to increased focusing
10 of particulate Mn oxides precipitated during inflow events with water depth, combined with a
11 high alkalinity in the deep basins linked to organic matter degradation by sulfate reduction.
12 Increased focusing of Mn oxides with water depth has been observed in other marine systems
13 (e.g. Slomp et al., 1997) and high alkalinity in sulfate-bearing organic rich sediments overlain
14 by an anoxic water column are typically linked to organic matter degradation through sulfate
15 reduction (Bernier et al., 1970).

16 Our microanalysis results show that the Mn carbonate enrichments at site LL19 are highly
17 laminar in character, implying rapid precipitation at or near the sediment-water interface.
18 Furthermore, these Mn carbonate enrichments occur independently of enrichments in Mo and
19 S. Sedimentary Mo can be used as a proxy for sulfidic conditions close to the sediment-water
20 interface, due to the conversion of seawater oxymolybdate to particle-reactive thiomolybdate
21 in the presence of hydrogen sulfide (Erickson and Helz, 2000). Although the ultimate burial
22 phase of Mo in sulfidic sediments is still debated (e.g., Helz et al., 2011), Mo concentrations
23 have successfully been used to reconstruct the redox history of the bottom water in restricted
24 coastal basins (Adelson et al., 2001; Jilbert and Slomp, 2013a). Sulfur enrichments in
25 sediments are typically associated with Fe-sulfides (Boesen and Postma, 1988), and thus are
26 also indicative of sulfidic conditions close to the sediment-water interface. The independence
27 of Mn enrichments from those of Mo and S suggests relatively oxic conditions at the time of
28 Mn carbonate precipitation. Both lines of evidence support the interpretation of Mn carbonate
29 precipitation following inflow events (Sternbeck and Sohlenius, 1997). Our age model
30 suggests that the two pronounced Mn carbonate layers at the base of the surface-sediment
31 block (Figure 5) correspond to inflows in 1993 and 1997 (Matthäus and Schinke, 1999).

1 Mn enrichments at the Landsort Deep site LD1 occur more frequently when compared to
2 other deep basin sites (Figure 4), as observed in earlier work (Lepland and Stevens, 1998). In
3 the Landsort Deep, Lepland and Stevens (1998) attributed the enrichments to the relatively
4 high alkalinity. Our pore water results show that alkalinity is similar to that of F80. However,
5 the pore water Mn^{2+} concentrations at the Landsort Deep site are much higher than elsewhere
6 ($>1 \mu M$ versus $<0.26 mM$ of Mn^{2+}). This may be related to the fact that the Landsort Deep is
7 the deepest basin in the Baltic Sea and its geometry makes it an excellent sediment trap. As a
8 consequence, sediment deposition rates are much higher than in the other Deeps (Lepland and
9 Stevens, 1998; Mort et al., 2010). Results of the recent IODP expedition suggest that
10 deposition rates may even be more than a factor of 6 higher; (Expedition 347 Scientists,
11 2014). Sediment focusing is also expected to lead to a higher input of organic matter and Mn
12 oxides to this basin. Given that rates of mineral dissolution are expected to depend on the
13 amount of material present, corresponding rates of input and dissolution of Mn oxide minerals
14 in the sediment are likely higher in the Landsort Deep than at other sites. Thus, we suggest
15 that differences in focusing of the sediment may explain the observed differences in pore
16 water chemistry and Mn sequestration. The differences in pore water chemistry will also
17 likely impact the exact solid phases formed in the sediments of the various deep basins.

18 The high-resolution analyses for the Landsort Deep site (LD1) also show that, besides Mn
19 carbonate enrichments, there are several distinct layers of Mn sulfide in the surface sediments
20 (Figure 5). These appear to coincide with enrichments in Mo, suggesting formation of Mn
21 sulfides during intervals of more reducing conditions (Mort et al., 2010). Furthermore, we
22 observe simultaneous enrichments of Br (Figure 5), which suggests higher organic carbon
23 contents (Ziegler et al., 2008). These results could imply that increased rates of sulfate
24 reduction linked to elevated inputs of organic material to the sediments drive the formation of
25 Mn sulfide. We note that the interval presented in the XRF map covers only a few years of
26 sediment accumulation, possibly suggesting rapid changes in Mn mineralogy in response to
27 seasonal variability of the organic matter flux (Figure 5). Primary productivity in the Baltic
28 Sea is known to vary seasonally (Bianchi et al., 2002; Fennel, 1995). Further work is required
29 to determine conclusively the mechanisms of MnS formation. While the presence of MnS has
30 been shown for the earlier anoxic time intervals in the Baltic (Böttcher and Huckriede, 1997;
31 Lepland and Stevens, 1998), this is the first time Mn sulfides are reported for such near-
32 surface sediments in the Baltic Sea.

1 The contrasting controls on Mn mineral formation in the Landsort Deep, compared to the
2 other deep basin sites, are further illustrated by a comparison of the trends in total Mn and Mo
3 concentrations (Figure 4) with measured bottom water oxygen concentrations for the period
4 1955 to 2010 (ICES Dataset on Ocean Hydrography 2014) for sites in the northern Gotland
5 Basin (LL19) and the Landsort Deep (LD1) (Figure 7). At site LL19, Mn enrichments in the
6 sediments coincide with low values of Mo in the sediment and inflows of oxygenated water.
7 This suggests that Mn burial is enhanced under more oxygenated bottom water conditions. At
8 LD1, in contrast, high Mn contents are observed from 1965 onwards, independent of inflows,
9 with the highest Mn values coinciding with periods with the highest sulfide concentrations
10 that occur in particular since the year 2000. This supports our hypothesis that the formation of
11 Mn carbonate minerals in the Landsort Deep is not always related to inflows and that the Mn
12 oxide supply is higher and more continuous when compared to the other basins.

13 **4.3 Changes in Mn burial linked to expanding hypoxia**

14 Strikingly, the more reducing conditions in the Gotland Basin (LL19, BY15) and Fårö Deep
15 sites (F80) over the past decades, as recorded in the Mo profiles (Figures 4 and 7), are
16 accompanied by a strong reduction in sediment Mn burial. Given the suggested link between
17 Mn burial and inflows, it is important to assess the occurrence of these inflows. During the
18 past two decades, there were two major (1993, 2003) and several minor inflow events (e.g.
19 1997) into the Baltic Sea. The event in 1993 was one of the strongest in the last 60 years
20 (Matthäus et al., 2008) and the inflow of 2003 (Feistel et al., 2003) was weaker but still
21 significant enough to reoxygenate the bottom water of the deep basins (Figure 7). However, at
22 LL19, Mn sequestration in the sediment between 2000 and 2010 has been negligible and the
23 inflow in 2003 is not recorded as a Mn carbonate enrichment (Figure 7), whereas in the high
24 resolution geochemical analyses Mn layers are clearly visible in both the LA-ICP-MS and
25 micro-XRF scans (Figure 5) and can be linked to the inflows in 1993 and 1997. A similar
26 “missing” Mn carbonate layer was observed by Heiser et al. (2001) in the Gotland Deep and
27 attributed to re-dissolution of Mn carbonate linked to resuspension events and mixing of the
28 sediment into unsaturated bottom waters. However, our cores were clearly laminated and the
29 ^{210}Pb profiles also show no evidence for mixing. We therefore conclude that, with the
30 increased hypoxia and euxinia in the Baltic Sea, Mn oxides are no longer converted to stable
31 Mn carbonates following inflows.

1 The formation of Mn carbonates in Baltic Sea sediments is typically believed to be induced
2 by the high alkalinity linked to organic matter degradation combined with high Mn^{2+}
3 concentrations in the surface sediment upon dissolution of Mn oxides following inflows
4 (Lepland and Stevens, 1998). After an inflow, supersaturation with respect to Mn carbonates
5 is thus expected to be reached in the surface sediment and not only at depths below ca. 5-10
6 cm (Figure 3). But what can inhibit the formation of these Mn carbonates? One possibility is
7 that at high pore water sulfide concentrations, Mn sulfides form instead of Mn carbonates.
8 However, given that there is negligible Mn enrichment in the upper sediments of F80, BY15
9 and LL19 today, we can exclude that possibility. Mn carbonate formation could be reduced if
10 alkalinity declined, but alkalinity in the bottom waters of the Gotland Deep has in fact
11 increased recently (e.g. Ulfsbo et al., 2011). High phosphate concentrations in the surface
12 sediment may potentially negatively affect the rate of Mn carbonate formation (Mucci, 2004).
13 However, there is no evidence for a significant rise in dissolved phosphate in the pore water
14 of Gotland Basin sediments over the past decades (e.g. Carman and Rahm, 1997; Hille et al.,
15 2005; Jilbert et al., 2011). Alternatively, we hypothesize that the Mn oxides that are formed
16 following modern inflow events might be reductively dissolved faster than previously. As a
17 consequence, the Mn^{2+} released from the oxides could then escape to the overlying water
18 instead of being precipitated in the form of Mn carbonate. This is in line with the results of
19 the simple diagenetic model where high rates of Mn oxide reduction lead to less Mn
20 carbonate formation (Figure 6).

21 There are multiple possible reductants for Mn oxides in marine sediments, including sulfide,
22 Fe^{2+} (e.g. Canfield and Thamdrup, 2009), NH_4^+ (e.g. Luther et al., 1997), and CH_4 (Beal et al.,
23 2009), with the role of the latter two reductants in marine sediments still being debated. Given
24 that the Fe^{2+} and CH_4 concentrations in the pore waters of the surface sediments of the
25 Gotland Basin area are negligible, these constituents are unlikely to play an important role as
26 a reductant for Mn oxides in the northern Gotland Basin (LL19), Fårö Deep (F80) and
27 Gotland Deep (BY15) sites. Furthermore, there is no evidence for a major recent change in
28 pore water CH_4 concentrations in the surface sediments. There is evidence, however, for a
29 recent rise in the bottom water sulfide concentrations in the deep basins of the Baltic Sea
30 (Figure 7) linked to eutrophication (Carstensen et al., 2014). As shown for the northern
31 Gotland Basin site (LL19), the more persistent presence of high concentrations of bottom
32 water sulfide and enrichments in sediment Mo, coincide with the decline in Mn in the
33 sediment (Figure 7).

1 We hypothesize that Mn oxides that are formed following modern inflow events and that are
2 deposited on the seafloor (Heiser et al., 2001) are no longer being converted to Mn carbonates
3 because of higher ambient concentrations of sulfide in the bottom water and in the pore water.
4 These higher sulfide concentrations are likely the direct result of increased sulfate reduction
5 driven by the ongoing rise in productivity in the Baltic Sea (Gustafsson et al., 2012;
6 Carstensen et al., 2014). The observed decline in Fe/Al at our deep basin sites (Figure 3)
7 suggests more muted shuttling of Fe oxides from shelves to the deeps linked to the expanding
8 hypoxia (e.g. Scholz et al., 2014) which may have reduced the buffer capacity of the
9 sediments for sulfide (e.g. Diaz and Rosenberg, 2008).

10 The rate of reduction of Mn oxides with sulfides is assumed to linearly depend on the
11 concentration of sulfide according to the following rate law (Wang and Van Cappellen, 1996):

$$12 \quad R = k C_{TS} C_{Mn\text{oxides}} \quad (6)$$

13 where k is a rate constant (with a value $<10^8 \text{ yr}^{-1}$) and C_{TS} stands for the total sulfide
14 concentration, i.e. the sum of the concentrations of H_2S and HS^- (in M). In our modeling
15 approach, the rate law for this process is assumed equal to

$$16 \quad R = k_{\text{red}} C_{Mn\text{oxides}} \quad (7)$$

17 Thus, if sulfide is the reductant, k_{red} can be assumed to be equivalent to the product of k and
18 C_{TS} . Sulfide will be absent in oxygenated pore waters, i.e. can be below $1 \mu\text{M}$ in the surface
19 sediment, but also can range up to 1.1 to 2.2 mM as observed at sites F80 and LD1 (Figure 2;
20 Appendix B). Corresponding k_{red} values for surface sediments in the Baltic Sea would then be
21 expected to range over 3-4 orders of magnitude and stay below 10^5 yr^{-1} , which is in line with
22 our assumptions. Mn carbonate formation is found to critically depend on the value of k_{red}
23 (Figure 6). While we are aware that other factors than the availability of Mn are also critical
24 to Mn carbonate formation, these model results do provide support to our suggestion that a
25 recent rise in sulfide concentrations in the pore waters and bottom waters may have made the
26 surface sediments more hostile to the preservation of Mn oxide after an inflow and might
27 contribute to their reduction. More Mn^{2+} could then escape to the overlying water instead of
28 being precipitated in the form of Mn carbonate, explaining the lack of recent Mn enrichments.

1 **4.4 Implications for Mn as a redox proxy**

2 In the classic model of Calvert and Pedersen (1993), Mn enrichments in sediments are
3 indicative of either permanent or temporary oxygenation of bottom waters. Sediments of
4 permanently anoxic basins, in contrast, are assumed to have no authigenic Mn enrichments
5 because there is no effective mechanism to concentrate the Mn oxides. Our results for the
6 Gotland Deep area indicate that the temporary oxygenation of the basin linked to inflows is
7 no longer recorded as a Mn enrichment in the recent sediment when hypoxia becomes basin-
8 wide. Thus, a decline in Mn burial (or a complete lack of Mn) in geological deposits in
9 combination with indicators for water column euxinia such as elevated Mo contents may
10 point towards expanding hypoxia, but does not exclude temporary oxygenation events.
11 Strikingly, only very little Mn was buried at sites F80 and LL19 during the previous period of
12 hypoxia in the Baltic Sea during the Medieval Climate Anomaly (Jilbert and Slomp, 2013b)
13 as well as at the end of the Holocene Thermal Maximum at site LL19 (Lenz et al., 2014). This
14 may be in line with hypoxia that was equally intense and widespread in the basin at the time
15 as it is today. Our results for the Landsort Deep suggests that Mn enrichments may also form
16 frequently in an anoxic basin as Mn carbonates and sulfides if the input of Mn from the
17 surrounding area is exceptionally high due to sediment focusing. Mn enrichments in
18 geological deposits thus can be indicative of both oxic and anoxic depositional environments,
19 emphasizing the need for multiple redox proxies.

20 **5 Conclusions**

21 We show that the most recent sediments in the Fårö Deep and Gotland Deep contain low
22 concentrations of Mn near the sediment surface. We hypothesize that this is due to the
23 expansion of the area with hypoxic bottom waters and the development of more continuous
24 bottom water euxinia over the past decades, linked to ongoing eutrophication and possibly
25 due to the reduced input of Fe-oxides that can act as a sink for sulfide. The high ambient
26 sulfide concentrations in the sediment and water column after an inflow event are suggested
27 to contribute to conditions that are conducive to faster dissolution of Mn oxides, leading to
28 less formation of Mn carbonates and more loss of Mn^{2+} to the water column. Our hypothesis
29 is supported by the results of a simple diagenetic model for Mn. It is also in accordance with
30 the general interpretation of sediment records of Mn in paleoceanography and the use of Mn
31 as a redox proxy where absence of Mn carbonates in sediments is assumed to be indicative of
32 euxinic bottom waters (e.g. Calvert and Pedersen, 1993). In the Landsort Deep, in contrast,

1 Mn sulfides and carbonates are still being precipitated. This could be due to strong focusing
2 of Mn rich sediment particles and high rates of sediment accumulation in the Landsort Deep.
3 Our results indicate that sediment Mn carbonates in the other deep basins of Baltic Sea no
4 longer reliably and consistently record inflows of oxygenated North Sea water. This has
5 implications for the use of Mn enrichments as a redox proxy when analyzing geological
6 deposits.

7 **Acknowledgements**

8 This work was funded by grants from the Baltic Sea 2020 foundation, the Netherlands
9 Organisation for Scientific Research (NWO Vidi and Vici), Utrecht University (via UU short
10 stay fellowship 2011), the EU-BONUS project HYPER and the European Research Council
11 under the European Community's Seventh Framework Programme for ERC Starting Grant
12 #278364. MW acknowledges Natural Environment Research Council [fellowship
13 #NE/J018856/1]. We thank the captain and crew of RV Skagerrak (2007), RV Aranda (2009),
14 RV Heincke (2010) and RV Pelagia (2011) and all participants of the cruises for their
15 assistance with the field work. We thank Simon Veldhuijzen for his contribution to the
16 analyses for site F80.

17

1 **References**

- 2 Adelson, J. M., Helz, G. R., and Miller, C. V.: Reconstructing the rise of recent coastal
3 anoxia; molybdenum in Chesapeake Bay sediments, *Geochim Cosmochim Acta*, 65, 237-252,
4 2001.
- 5 Ahl, T.: River Discharges of Fe, Mn, Cu, Zn, and Pb into the Baltic Sea from Sweden, *Ambio*
6 *Special Report*, 219-228, 1977.
- 7 Appleby, P. and Oldfield, F.: The assessment of ²¹⁰Pb data from sites with varying sediment
8 accumulation rates, *Hydrobiology*, 103, 29-35, 1983.
- 9 Beal, E. J., House, C. H., and Orphan, V. J.: Manganese- and Iron-Dependent Marine
10 Methane Oxidation, *Science*, 325, 184-187, 2009.
- 11 Berner, R. A.: *Early diagenesis: A theoretical approach*, Princeton University Press, 1980.
- 12 Berner, R. A., Scott, M. R. and Thomlinson, C.: Carbonate alkalinity in the pore waters of
13 anoxic marine sediments, *Limnol. Oceanogr.* 15(4), 544-549, 1970.
- 14 Bianchi, T. S., Rolff, C., Widbom, B., and Elmgren, R.: Phytoplankton Pigments in Baltic Sea
15 Seston and Sediments: Seasonal Variability, Fluxes, and Transformations, *Estuar Coast Shelf*
16 *Sci*, 55, 369-383, 2002.
- 17 Boesen, C. and Postma, D.: Pyrite formation in anoxic environments of the Baltic, *Am J Sci*,
18 288, 575-603, 1988.
- 19 Böttcher, M. E. and Huckriede, H.: First occurrence and stable isotope composition of
20 authigenic γ -MnS in the central Gotland Deep (Baltic Sea), *Mar Geol*, 137, 201-205, 1997.
- 21 Boudreau, B. P.: *Diagenetic models and their implementation: modelling transport and*
22 *reactions in aquatic sediments*, Springer Berlin, 1997.
- 23 Cai, W.-J and Reiners, C. E.: The development of pH and pCO₂ microelectrodes for studying
24 the carbonate chemistry of pore waters near the sediment-water interface, *Limnol. Oceanogr.*,
25 38(8), 1762-1773, 1993.
- 26 Calvert, S. and Pedersen, T.: Geochemistry of recent oxic and anoxic marine sediments:
27 Implications for the geological record, *Mar Geol*, 113, 67-88, 1993.
- 28 Calvert, S. and Pedersen, T.: Sedimentary geochemistry of manganese; implications for the
29 environment of formation of manganese black shales, *Econ Geol*, 91, 36-47, 1996.

1 Canfield, D. E. and Thamdrup, B.: Towards a consistent classification scheme for
2 geochemical environments, or, why we wish the term 'suboxic' would go away, *Geobiology*,
3 7, 385-392, 2009.

4 Carman, R. and Rahm, L.: Early diagenesis and chemical characteristics of interstitial water
5 and sediments in the deep deposition bottoms of the Baltic proper, *J Sea Res*, 37, 25-47, 1997.

6 Carstensen, J., Andersen, J. H., Gustafsson, B. G., and Conley, D. J.: Deoxygenation of the
7 Baltic Sea during the last century, *PNAS* 111, 5628-5633, 2014.

8 Conley, D. J., Björck, S., Bonsdorff, E., Carstensen, J., Destouni, G., Gustafsson, B. G.,
9 Hietanen, S., Kortekaas, M., Kuosa, H., Meier, H. E., Müller-Karulis, B., Nordberg, K.,
10 Norkko, A., Nürnberg, G., Pitkänen, H., Rabalais, N. N., Rosenberg, R., Savchuk, O. P.,
11 Slomp, C. P., Voss, M., Wulff, F., and Zillen, L.: Hypoxia-related processes in the Baltic Sea,
12 *Environ Sci Technol*, 43, 3412-3420, 2009.

13 Dellwig, O., Leipe, T., März, C., Glockzin, M., Pollehne, F., Schnetger, B., Yakushev, E. V.,
14 Böttcher, M. E., and Brumsack, H.-J.: A new particulate Mn-Fe-P-shuttle at the redoxcline of
15 anoxic basins, *Geochim Cosmochim Acta*, 74, 7100-7115, 2010.

16 Dellwig, O., Schnetger, B., Brumsack, H.-J., Grossart, H.-P., and Umlauf, L.: Dissolved
17 reactive manganese at pelagic redoxclines (part II): Hydrodynamic conditions for
18 accumulation, *J Mar Syst*, 90, 31-41, 2012.

19 Diaz, R. J. and Rosenberg, R.: Marine benthic hypoxia: a review of its ecological effects and
20 the behavioural responses of benthic macrofauna, *Oceanography and marine biology. An*
21 *annual review*, 33, 245-203, 1995.

22 Emerson, S., Jacobs, L., and Tebo, B.: The Behavior of Trace Metals in Marine Anoxic
23 Waters: Solubilities at the Oxygen-Hydrogen Sulfide Interface. In: *Trace Metals in Sea*
24 *Water*, Wong, C. S., Boyle, E., Bruland, K., Burton, J. D., and Goldberg, E. (Eds.), NATO
25 *Conference Series*, Springer US, 1983.

26 Erickson, B. E. and Helz, G. R.: Molybdenum(VI) speciation in sulfidic waters: Stability and
27 lability of thiomolybdates, *Geochim Cosmochim Acta*, 64, 1149-1158, 2000.

28 Expedition 347 Scientists: Baltic Sea Basin Paleoenvironment: paleoenvironmental evolution
29 of the Baltic Sea Basin through the last glacial cycle. *IODP Prel. Rept.*, 347, 2014.
30 doi:10.2204/iodp.pr.347.2014

- 1 Feistel, R., Nausch, G., Mohrholz, V., Lysiak-Pastuszak, E., Seifert, T., Matthaus, W.,
2 Kruger, S., and Hansen, I. S.: Warm waters of summer 2002 in the deep Baltic Proper,
3 *Oceanologia*, 45, 571-592, 2003.
- 4 Fennel, W.: A model of the yearly cycle of nutrients and plankton in the Baltic Sea, *J Mar*
5 *Syst*, 6, 313-329, 1995.
- 6 Fonselius, S. and Valderrama, J.: One hundred years of hydrographic measurements in the
7 Baltic Sea, *J Sea Res*, 49, 229-241, 2003.
- 8 Gustafsson, B. G., Schenk, F., Blenckner, T., Eilola, K., Meier, H. M., Müller-Karulis, B.,
9 Neumann, T., Ruoho-Airola, T., Savchuk, O. P., and Zorita, E.: Reconstructing the
10 development of Baltic Sea eutrophication 1850–2006, *Ambio*, 41, 534-548, 2012.
- 11 Heiser, U., Neumann, T., Scholten, J., and Stüben, D.: Recycling of manganese from anoxic
12 sediments in stagnant basins by seawater inflow: A study of surface sediments from the
13 Gotland Basin, Baltic Sea, *Mar Geol*, 177, 151-166, 2001.
- 14 Helz, G. R., Bura-Nakić, E., Mikac, N., and Ciglencčki, I.: New model for molybdenum
15 behavior in euxinic waters, *Chem Geol*, 284, 323-332, 2011.
- 16 Hille, S., Nausch, G., and Leipe, T.: Sedimentary deposition and reflux of phosphorus (P) in
17 the Eastern Gotland Basin and their coupling with P concentrations in the water column,
18 *Oceanologia*, 47, 663-679, 2005.
- 19 Holtermann, P. L. and Umlauf, L.: The Baltic Sea Tracer Release Experiment: 2. Mixing
20 processes, *Journal of Geophysical Research: Oceans*, 117, C01022, 2012.
- 21 Huckriede, H. and Meischner, D.: Origin and environment of manganese-rich sediments
22 within black-shale basins, *Geochim Cosmochim Acta*, 60, 1399-1413, 1996.
- 23 Huerta-Diaz, M. A. and Morse, J. W.: Pyritization of trace metals in anoxic marine sediments,
24 *Geochim Cosmochim Acta*, 56, 2681-2702, 1992.
- 25 ICES Dataset on Ocean Hydrography. The International Council for the Exploration of the
26 Sea, Copenhagen. 2014.
- 27 Jacobs, L., Emerson, S., and Skei, J.: Partitioning and transport of metals across the O₂/H₂S
28 interface in a permanently anoxic basin: Framvaren Fjord, Norway, *Geochim Cosmochim*
29 *Acta*, 49, 1433-1444, 1985.

- 1 Jakobsen, R. and Postma, D.: Formation and solid solution behavior of Ca-rhodochrosites in
2 marine muds of the Baltic deeps, *Geochim Cosmochim Acta*, 53, 2639-2648, 1989.
- 3 Jilbert, T. and Slomp, C. P.: Iron and manganese shuttles control the formation of authigenic
4 phosphorus minerals in the euxinic basins of the Baltic Sea, *Geochim Cosmochim Acta*, 107,
5 155-169, 2013a.
- 6 Jilbert, T. and Slomp, C. P.: Rapid high-amplitude variability in Baltic Sea hypoxia during the
7 Holocene, *Geology*, 41, 1183-1186, 2013b
- 8 Jilbert, T., Slomp, C. P., Gustafsson, B. G., and Boer, W.: Beyond the Fe-P-redox connection:
9 preferential regeneration of phosphorus from organic matter as a key control on Baltic Sea
10 nutrient cycles, *Biogeosciences*, 8, 1699-1720, 2011.
- 11 Jochum, K. P., Weis, U., Stoll, B., Kuzmin, D., Yang, Q., Raczek, I., Jacob, D. E., Stracke,
12 A., Birbaum, K., and Frick, D. A.: Determination of reference values for NIST SRM 610–617
13 glasses following ISO guidelines, *Geostand Geoanal Res*, 35, 397-429, 2011.
- 14 Jones, C., Crowe, S. A., Sturm, A., Leslie, K., MacLean, L., Katsev, S., Henny, C., Fowle, D.
15 A., and Canfield, D. E.: Biogeochemistry of manganese in ferruginous Lake Matano,
16 Indonesia, *Biogeosciences*, 8, 2977-2991, 2011.
- 17 Katsikopoulos, D., Fernández-González, A. and Prieto, M.: Precipitation and mixing
18 properties of the “disordered” (Mn,Ca)CO₃ solid solution, *Geochim Cosmochim Acta* 73,
19 6147-6161, 2009.
- 20 Kulik, D. A., Kersten, M., Heiser, U. and Neumann, T.: Application of Gibbs Energy
21 Minimization to Model Early-Diagenetic Solid-Solution Aqueous-Solution Equilibria
22 Involving Authigenic Rhodochrosites in Anoxic Baltic Sea Sediments, *Aquatic Geochemistry*
23 6, 147-199, 2000.
- 24 Lenz, C., Behrends, T., Jilbert, T., Silveira, M., and Slomp, C. P.: Redox-dependent changes
25 in manganese speciation in Baltic Sea sediments from the Holocene Thermal Maximum: An
26 EXAFS, XANES and LA-ICP-MS study, *Chem Geol*, 370, 49-57, 2014.
- 27 Lepland, A. and Stevens, R. L.: Manganese authigenesis in the Landsort Deep, Baltic Sea,
28 *Mar Geol*, 151, 1-25, 1998.

- 1 Löffler, A.: The importance of particles for the distribution of trace metals in the Baltic Sea,
2 especially under changing redox conditions in the central Baltic deep basins.,
3 *Meereswissenschaftliche Berichte Warnemünde*, 27, 153, 1997.
- 4 Luther III, G. W., Rickard, D. T., Theberge, S., and Olroyd, A.: Determination of metal (bi)
5 sulfide stability constants of Mn²⁺, Fe²⁺, Co²⁺, Ni²⁺, Cu²⁺, and Zn²⁺ by voltammetric
6 methods, *Environ Sci Technol*, 30, 671-679, 1996.
- 7 Luther III, G. W., Sundby, B., Lewis, B. L., Brendel, P. J., and Silverberg, N.: Interactions of
8 manganese with the nitrogen cycle: Alternative pathways to dinitrogen, *Geochim Cosmochim*
9 *Acta*, 61, 4043-4052, 1997.
- 10 Lyons, T. W. and Severmann, S.: A critical look at iron paleoredox proxies: New insights
11 from modern euxinic marine basins, *Geochim Cosmochim Acta*, 70, 5698-5722, 2006.
- 12 MacDonald, R. W. and Gobeil, C.: Manganese sources and sinks in the Arctic Ocean with
13 reference to periodic enrichments in basin sediments, *Aquat Geochem*, 18, 565-591, 2012.
- 14 Madison, A. S., Tebo, B. M., and Luther, G. W.: Simultaneous determination of soluble
15 manganese (III), manganese (II) and total manganese in natural (pore) waters, *Talanta*, 84,
16 374-381, 2011.
- 17 Manheim, F. T.: A geochemical profile in the Baltic Sea, *Geochim Cosmochim Acta*, 25, 52-
18 70, 1961.
- 19 Martin, J.-M. and Meybeck, M.: Elemental mass-balance of material carried by major world
20 rivers, *Mar Chem*, 7, 173-206, 1979.
- 21 Matthäus, W. and Schinke, H.: The influence of river runoff on deep water conditions of the
22 Baltic Sea, *Hydrobiologia*, 393, 1-10, 1999.
- 23 Matthäus, W. and Franck, H.: Characteristics of major Baltic inflows--a statistical analysis,
24 *Cont Shelf Res*, 12, 1375-1400, 1992.
- 25 Matthäus, W., Nehring, D., Feistel, R., Nausch, G., Mohrholz, V., and Lass, H.-U.: The
26 Inflow of Highly Saline Water into the Baltic Sea. In: *State and Evolution of the Baltic Sea,*
27 1952–2005, John Wiley & Sons, Inc., 2008.
- 28 Meister, P., Bernasconi, S. M., Aiello, I. W., Vasconcelos, C., and McKenzie, J. A.: Depth
29 and controls of Ca-rhodochrosite precipitation in bioturbated sediments of the Eastern

1 Equatorial Pacific, ODP Leg 201, Site 1226 and DSDP Leg 68, Site 503, *Sedimentology*, 56,
2 1552-1568, 2009.

3 Mort, H. P., Slomp, C. P., Gustafsson, B. G., and Andersen, T. J.: Phosphorus recycling and
4 burial in Baltic Sea sediments with contrasting redox conditions, *Geochim Cosmochim Acta*,
5 74, 1350-1362, 2010.

6 Mouret, A., Anschutz, P., Lecroart, P., Chaillou, G., Hyacinthe, C., Deborde, J., Jorissen, F.,
7 Deflandre, B., Schmidt, S., and Jouanneau, J.-M.: Benthic geochemistry of manganese in the
8 Bay of Biscay, and sediment mass accumulation rate, *Geo-Mar Lett*, 29, 133-149, 2009.

9 Mucci, A.: The behavior of mixed Ca–Mn carbonates in water and seawater: controls of
10 manganese concentrations in marine porewaters, *Aquat Geochem*, 10, 139-169, 2004.

11 Neretin, L. N., Pohl, C., Jost, G., Leipe, T., and Pollehne, F.: Manganese cycling in the
12 Gotland Deep, Baltic Sea, *Mar Chem*, 82, 125-143, 2003.

13 Neumann, T., Christiansen, C., Clasen, S., Emeis, K.-C., and Kunzendorf, H.: Geochemical
14 records of salt-water inflows into the deep basins of the Baltic Sea, *Cont Shelf Res*, 17, 95-
15 115, 1997.

16 Neumann, T., Heiser, U., Leosson, M. A., and Kersten, M.: Early diagenetic processes during
17 Mn-carbonate formation: Evidence from the isotopic composition of authigenic Ca-
18 rhodochrosites of the Baltic Sea, *Geochim Cosmochim Acta*, 66, 867-879, 2002.

19 Pakhomova, S. and Yakushev, E. V.: Manganese and Iron at the Redox Interfaces in the
20 Black Sea, the Baltic Sea, and the Oslo Fjord. In: *Chemical Structure of Pelagic Redox*
21 *Interfaces*, Yakushev, E. V. (Ed.), *The Handbook of Environmental Chemistry*, Springer
22 Berlin Heidelberg, 2013.

23 Pakhomova, S. V., Hall, P. O., Kononets, M. Y., Rozanov, A. G., Tengberg, A., and
24 Vershinin, A. V.: Fluxes of iron and manganese across the sediment–water interface under
25 various redox conditions, *Mar Chem*, 107, 319-331, 2007.

26 Parkhurst, D. L. and Appelo, C.: User's guide to PHREEQC (Version 2): A computer program
27 for speciation, batch-reaction, one-dimensional transport, and inverse geochemical
28 calculations, US Geological Survey Water-Resources Investigations Report 99-4259, 312 pp.,
29 1999.

- 1 Passier, H. F., Böttcher, M. E., and de Lange, G. J.: Sulphur enrichment in organic matter of
2 eastern mediterranean sapropels: A study of sulphur isotope partitioning, *Aquat Geochem*, 5,
3 99-118, 1999.
- 4 Pohl, C. and Hennings, U.: The coupling of long-term trace metal trends to internal trace
5 metal fluxes at the oxic–anoxic interface in the Gotland Basin (57° 19, 20' N; 20° 03, 00' E)
6 Baltic Sea, *J Mar Syst*, 56, 207-225, 2005.
- 7 Rickard, D.: The solubility of FeS, *Geochim Cosmochim Acta*, 70, 5779-5789, 2006.
- 8 Riley, J. P.: The Spectrophotometric Determination of Ammonia in Natural Waters with
9 Particular Reference to Sea-Water, *Anal Chim Acta*, 9, 575-589, 1953.
- 10 Savchuk, O. P., Wulff, F., Hille, S., Humborg, C., and Pollehne, F.: The Baltic Sea a century
11 ago—a reconstruction from model simulations, verified by observations, *J Mar Syst*, 74, 485-
12 494, 2008.
- 13 Scholz, F., McManus, J., and Sommer, S.: The manganese and iron shuttle in a modern
14 euxinic basin and implications for molybdenum cycling at euxinic ocean margins, *Chem*
15 *Geol*, 355, 56-68, 2013.
- 16 Scholz, F., McManus, J., Mix, A. C., Hensen, C., and Schneider, R. R.: The impact of ocean
17 deoxygenation on iron release from continental margin sediments, *Nat. Geosci.*, 7, 433-437,
18 2014.
- 19 Slomp, C. P., Malschaert, J. F. P., Lohse, L., and Van Raaphorst, W.: Iron and manganese
20 cycling in different sedimentary environments on the North Sea continental margin, *Cont*
21 *Shelf Res*, 17, 1083-1117, 1997.
- 22 Soetaert, K., Petzoldt, T., and Meysman, F.: Marelac: Tools for aquatic sciences. R Package
23 Version 2.1.3. 2010.
- 24 Soetaert, K. and Meysman, F.: Reactive transport in aquatic ecosystems: Rapid model
25 prototyping in the open source software R, *Environmental Modelling & Software*, 32, 49-60,
26 2012.
- 27 Sternbeck, J. and Sohlenius, G.: Authigenic sulfide and carbonate mineral formation in
28 Holocene sediments of the Baltic Sea, *Chem Geol*, 135, 55-73, 1997.
- 29 Strickland, J. D. H. and Parsons, T. R.: A practical handbook of seawater analysis, Fisheries
30 Research Board of Canada, Ottawa, Canada, 1972.

- 1 Suess, E.: Mineral phases formed in anoxic sediments by microbial decomposition of organic
2 matter, *Geochim Cosmochim Acta*, 43, 339-352, 1979.
- 3 Sundby, B., Silverberg, N., and Chesselet, R.: Pathways of manganese in an open estuarine
4 system, *Geochim Cosmochim Acta*, 45, 293-307, 1981.
- 5 Turnewitsch, R. and Pohl, C.: An estimate of the efficiency of the iron-and manganese-driven
6 dissolved inorganic phosphorus trap at an oxic/euxinic water column redoxcline, *Global*
7 *Biogeochem Cycles*, 24, GB4025, 2010.
- 8 Ulfso, A., Hulth, S., and Anderson, L. G.: pH and biogeochemical processes in the Gotland
9 Basin of the Baltic Sea, *Mar Chem*, 127, 20-30, 2011.
- 10 van Santvoort, P. J. M., De Lange, G. J., Thomson, J., Colley, S., Meysman, F. J. R., and
11 Slomp, C. P.: Oxidation and origin of organic matter in surficial eastern mediterranean
12 hemipelagic sediments, *Aquat Geochem*, 8, 153-175, 2002.
- 13 Wang, Y. and Van Cappellen, P.: A multicomponent reactive transport model of early
14 diagenesis: Application to redox cycling in coastal marine sediments, *Geochim Cosmochim*
15 *Acta*, 60, 2993-3014, 1996.
- 16 Yakushev, E. V., Kuznetsov, I. S., Podymov, O. I., Burchard, H., Neumann, T., and Pollehne,
17 F.: Modeling the influence of oxygenated inflows on the biogeochemical structure of the
18 Gotland Sea, central Baltic Sea: Changes in the distribution of manganese, *Comput Geosci*,
19 37, 398-409, 2011.
- 20 Yeats, P., Sundby, B., and Bewers, J.: Manganese recycling in coastal waters, *Mar Chem*, 8,
21 43-55, 1979.
- 22 Ziegler, M., Jilbert, T., de Lange, G. J., Lourens, L. J., and Reichart, G. J.: Bromine counts
23 from XRF scanning as an estimate of the marine organic carbon content of sediment cores,
24 *Geochem Geophys Geosy*, 9, Q05009, 2008.
- 25 Zillén, L., Lenz, C., and Jilbert, T.: Stable lead (Pb) isotopes and concentrations – A useful
26 independent dating tool for Baltic Sea sediments, *Quat Geochronol*, 8, 41-45, 2012.
- 27
- 28

1 Table 1. Characteristics of the 8 study sites in the Baltic Sea. Redox: bottom water redox
 2 conditions at the time of sampling. Pore water samples were obtained during every cruise and
 3 were similar between years at each station. Here, the most complete data sets for each station
 4 are presented. Average sedimentation rates for the last 30 years are based on ^{210}Pb dating.

Site name	Location	Cruise	Position	Water depth (m)	Sedimentation Rate (cm yr^{-1})	Redox	Salinity
Fladen	Fladen	R/V Skagerak Sept. 2007	57°11.57N 11°39.25E	82	1.0	oxic	34.2
LF1	Northern Gotland Basin	R/V Aranda May/June 2009	57°58.95N 21°16.84E	67	0.25	oxic	8.2
BY5	Bornholm Basin	R/V Skagerak Sept. 2007	55°15.16N 15°59.16E	89	0.23	$\text{O}_2=4.0$ μM	16.2
LF3	Eastern Gotland Basin	Sediment: R/V Aranda May/June 2009 Pore water: R/V Pelagia May 2011	57°59.50N 20°46.00E	95	0.50	$\text{H}_2\text{S}=2.9$ μM	10.1
LL19	Northern Gotland Basin	Sediment: R/V Aranda May/June 2009 Pore water: R/V Heincke July 2010	58°52.84N 20°18.65E	169	0.30	$\text{H}_2\text{S}=19.9$ μM	11.4
BY15	Gotland Deep	Sediment R/V Aranda May/June 2009 Pore water:	57°19.20N 20°03.00E	238	0.27	$\text{H}_2\text{S}=74.1$ μM	12.5

		R/V Heincke					
		July 2010					
F80	Fårö Deep	Sediment:	58°00.00N	191	0.55	H ₂ S=45.	12.0
		R/V Aranda	19°53.81E			6 µM	
		May/June					
		2009					
		Pore water:					
		R/V Heincke					
		July 2010					
LD1	Landsort Deep	R/V Pelagia	58°37.47N	416	0.77	anoxic	10.6
		May 2011	18°15.23E			and sulfidic	

1

1 Table 2. Diffusive fluxes of Mn across the sediment-water interface at all 6 sites. For further
 2 details, see text. For the bottom water and pore water data, see Appendix B.

Site	Location	Year and cruise	Depth range cm	Diffusive Mn flux $\mu\text{mol m}^{-2} \text{d}^{-1}$
LF1	Northern Gotland Basin	2009 R/V Aranda	BW-0.25	115
BY5	Bornholm Basin	2009 R/V Aranda	BW-0.5	236
LL19	Northern Gotland Basin	2009 R/V Aranda	BW-0.25	81
BY15	Gotland Deep	2009 R/V Aranda	BW-0.25	98
F80	Fårö Deep	2009 R/V Aranda	BW-0.25	84
LD1	Landsort Deep	2011R/V Pelagia	BW*-2.5	~220

3 * LD1 has no measured bottom water sample. Therefore, the flux was estimated using the
 4 bottom water value from the Landsort Deep site BY31 from Mort et al. 2010.

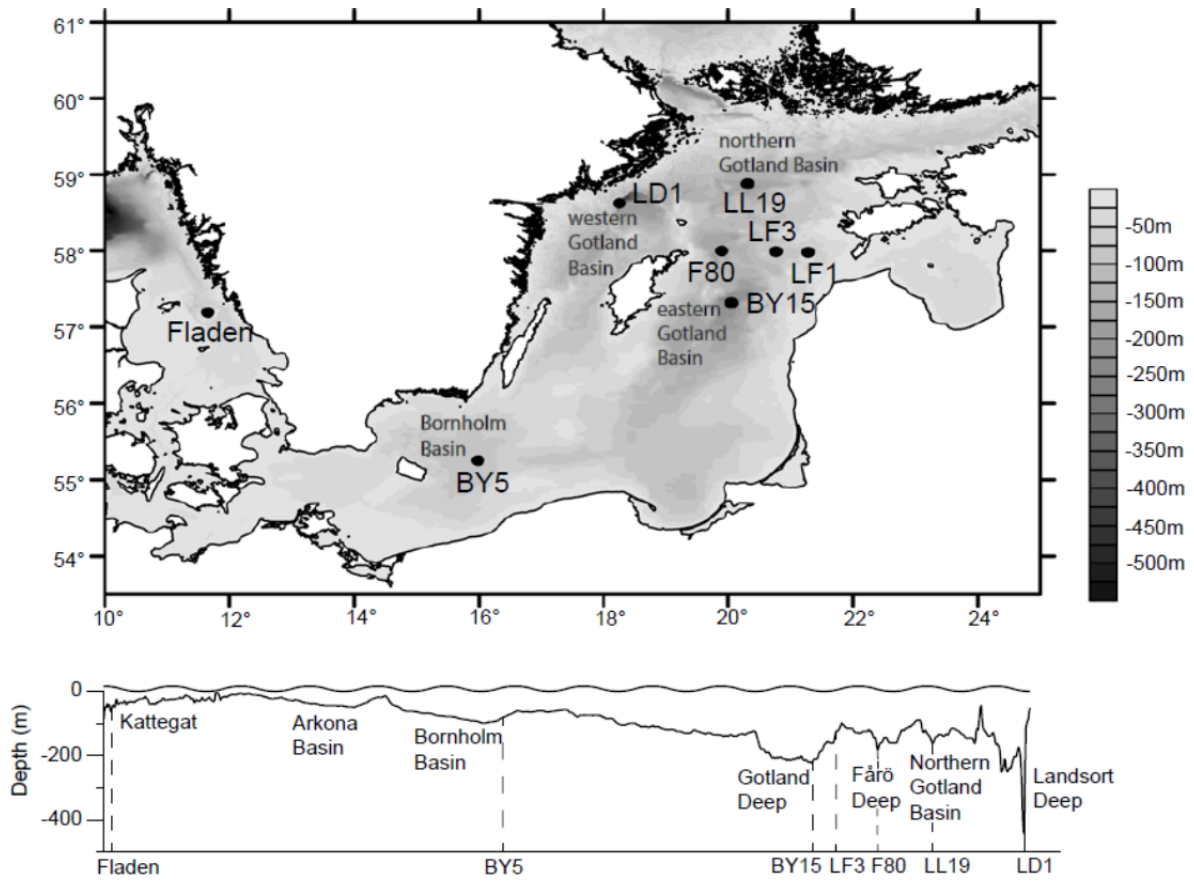
5

1 Table 3. Environmental parameters, boundary conditions (where $x=0$ refers to the sediment-
 2 water interface and $x = 1$ cm refers to a depth of 1 cm in the sediment) and first-order rate
 3 constants used in the simple diagenetic model for Mn for a “typical” Gotland basin sediment,
 4 including the sources, where relevant.

Environmental and transport Parameters	Value	Source
- Porosity (vol%)	99	Appendix B
- Temperature (°C)	5	Appendix B
- Salinity	12	Table 1
- Sedimentation rate (m yr^{-1})	0.0025	Table 1
Boundary condition at sediment water interface ($x=0$)*		
Fixed concentration, Mn^{2+} (mol m^{-3})	0	Typical for oxic waters
Fixed flux of MnCO_3 ($\text{mol m}^{-2} \text{y}^{-1}$)	0	Assuming all formation in the sediment
Transient flux of Mn oxides ($\text{mol m}^{-2} \text{y}^{-1}$)	4 months: 1, then 0	Section 4.1, 0.33 mol m^{-2} deposited in 4 months
Rate constants		
- k_{red} (yr^{-1})	Range of 0.1 to 1,000	Slomp et al (1997) & Wang & Van Cappellen (1996); see text
- k_{prec} (yr^{-1})	5,000	Wang & Van Cappellen (1996); see text

5 *For all chemical species a zero-gradient boundary condition was specified at the bottom of
 6 the model domain.

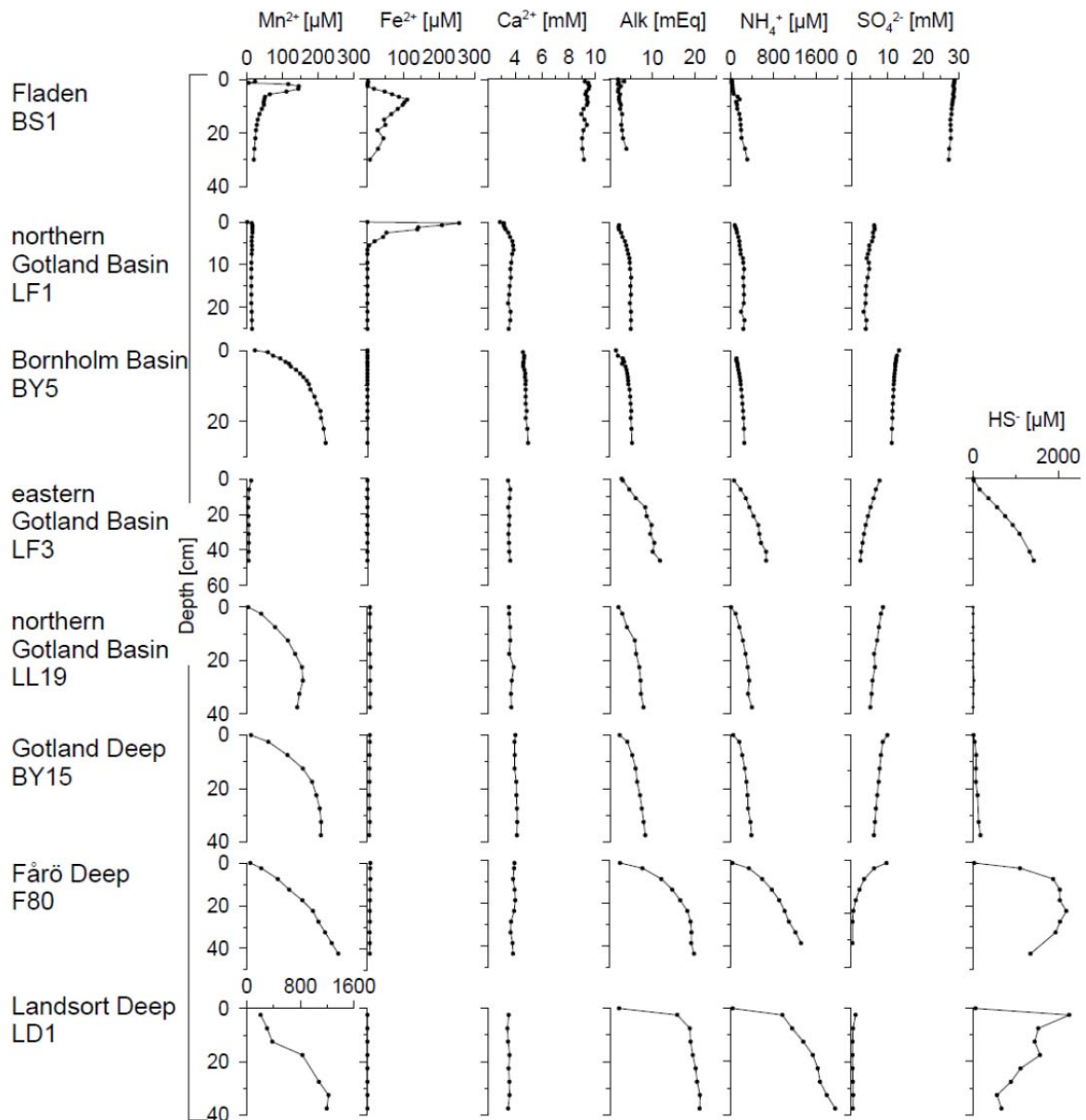
7



1

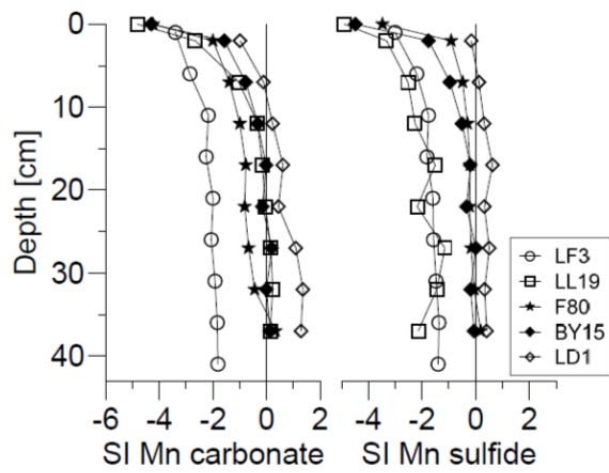
2 Figure 1 Bathymetric map and depth profile of the Baltic Sea showing the locations of the
 3 sampling sites.

4



1
 2 Figure 2 Pore water profiles of manganese (II), iron (Fe), calcium, alkalinity, ammonium and
 3 sulfate for all 8 sites and hydrogen sulfide for the 5 deepest sites. Note, that Fe^{2+} is below
 4 detection limit in core LF3 and LD1 and dissolved sulfide is expressed as HS^- , some H_2S can
 5 be present as well.

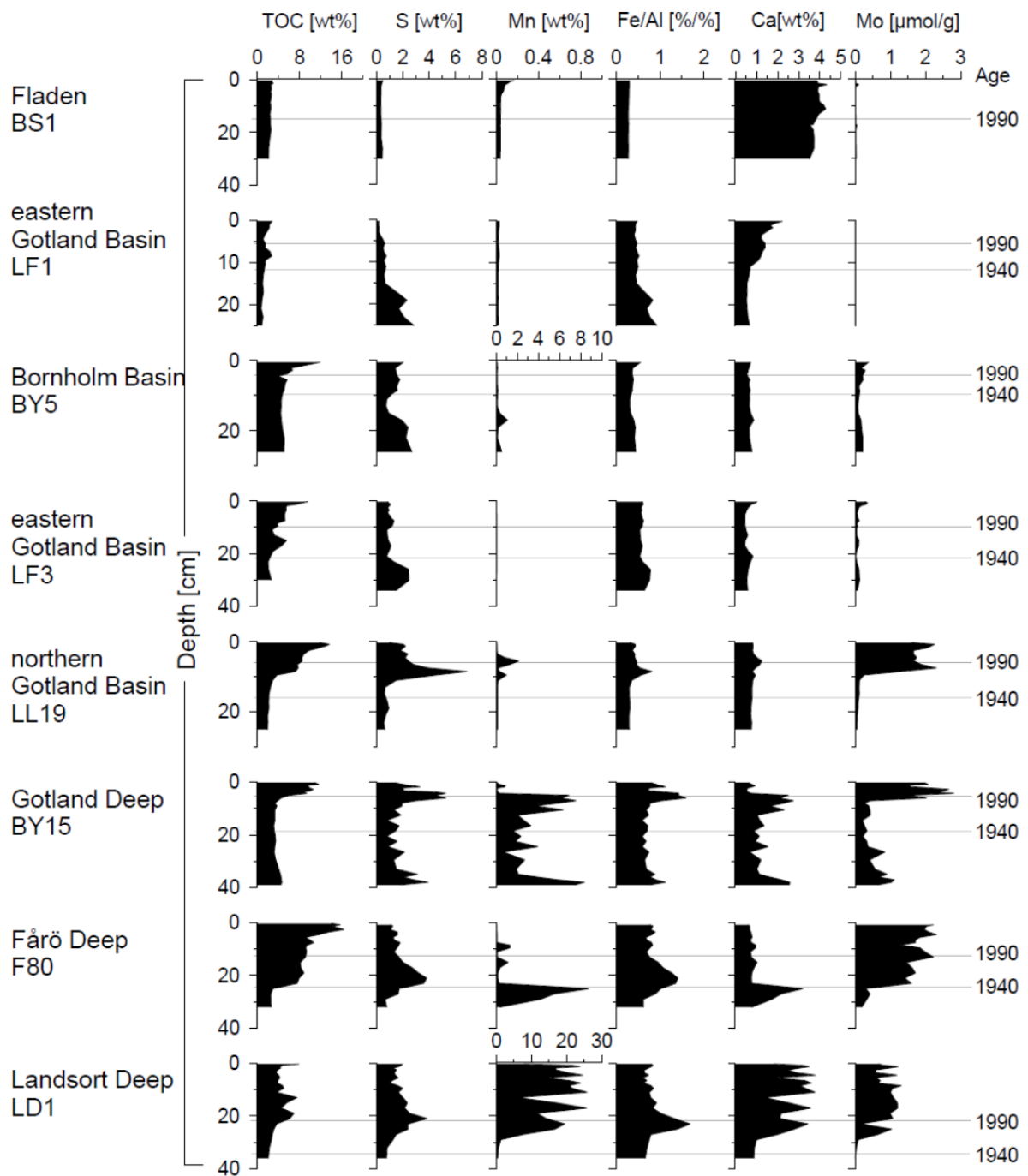
6



1

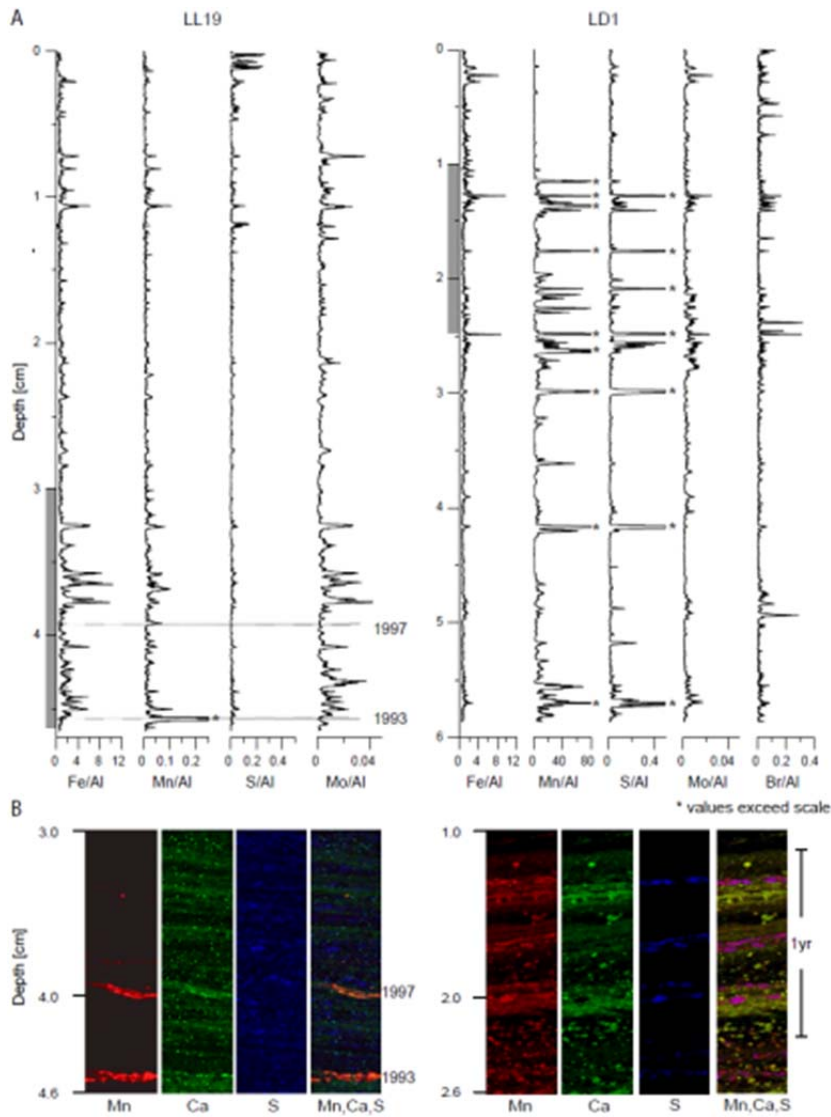
2 Figure 3 Saturation indices (SI) for Mn carbonate (here as $Mn_{0.74}Ca_{0.26}CO_3$) and Mn sulfide as
 3 calculated from the pore water data with PHREEQC.

4

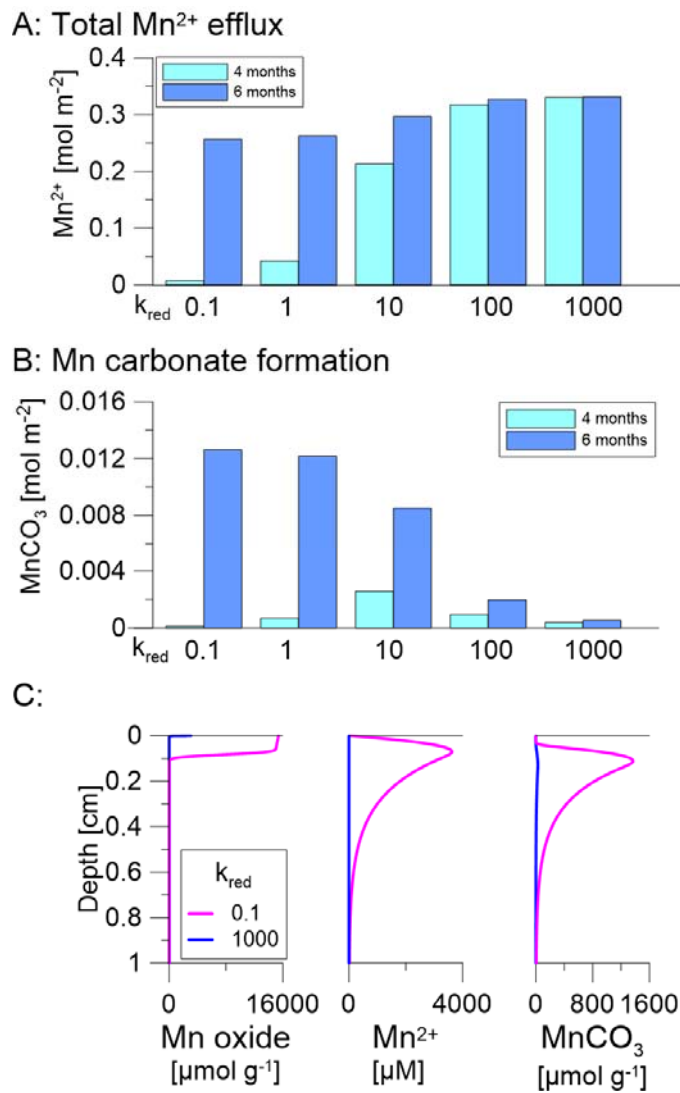


1
 2 Figure 4 Sediment depth profiles of total organic carbon (TOC), sulfur (S), manganese (Mn),
 3 iron to aluminum ratio (Fe/Al), calcium (Ca) and molybdenum for all 8 sites. Note the
 4 different scale for manganese at Fladen and LF1, and LD1. Grey lines indicate the years 1990
 5 and 1940, based on sediment dating. These date markers are used to demonstrate the
 6 variability of sedimentation rates in the study area.

7



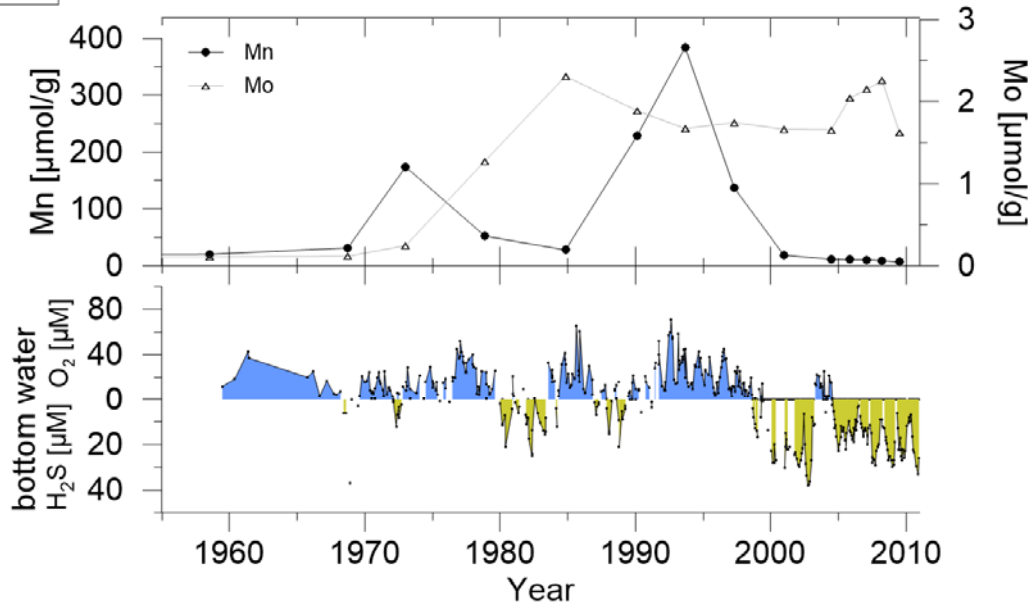
1
 2 Figure 5 A: High resolution elemental profiles of Fe/Al, Mn/Al, S/Al, Mo/Al and Br/Al (only
 3 LD1) generated by LA-ICP-MS line scanning for resin-embedded surface sediment blocks.
 4 Note the difference in absolute values for Mn/Al between LL19 and LD1. The depth scale
 5 refers to the compacted sediment in the resin blocks (the total length of wet sediment prior to
 6 embedding was 5.5 cm (LL19) and 11.3 cm (LD1)). Peaks marked with a * exceed the scale.
 7 B: Compilation of micro XRF maps for station LL19 and LD1 showing the distribution of
 8 manganese (red), calcium (green) and sulfur (blue) at the depth indicated by grey panels in the
 9 LA-ICP-MS line scans. Color intensity within each map is internally proportional to XRF
 10 counts, but relative scaling has been modified to highlight features. The fourth picture for
 11 each station shows a RGB (red-green-blue) composite of the three elements with orange to
 12 yellow colors indicating a mix of Mn and Ca, and therefore, representing Ca-Mn carbonates.
 13 The pink/purple represents a mix of Mn and S, hence Mn sulfide.



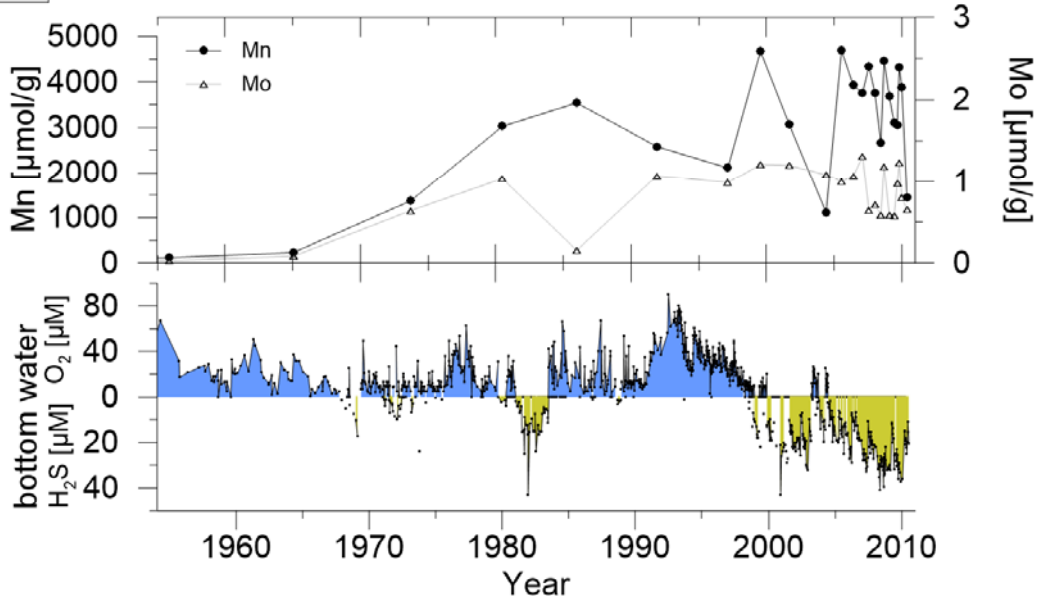
1
 2 Figure 6. A: Total sediment-water exchange of Mn²⁺ and B: integrated rates of Mn carbonate
 3 formation over the upper cm of the sediment (in mol m⁻²) for the first 4 months (with k_{red}
 4 either 0.1, 1, 10, 100 or 1000 yr⁻¹) and for the total 6 months (with k_{red} equal to 1000 yr⁻¹ to
 5 represent anoxia during the last two months of each simulation) as described in the text. C:
 6 Depth profiles of Mn oxide (after 4 months), Mn²⁺ at the start of the anoxic phase and MnCO₃
 7 (after 6 months) as calculated with the model in the same scenarios as A and B.

8

LL19



LD1



1
2 Figure 7 Records of sediment manganese and molybdenum for 1955-2010 for core LL19 and
3 core LD1 and corresponding bottom water oxygen and sulfide concentrations from
4 monitoring data (for LD1 the nearby monitoring station LL23 was used; ICES Dataset on
5 Ocean Hydrography, 2014).